Research Square

Preprints are preliminary reports that have not undergone peer review.
They should not be considered conclusive, used to inform clinical practice,
or referenced by the media as validated information.

Sequence stratigraphy, sedimentary systems and implications for hydrocarbon exploration in the Qaidam Basin, Northern China

Fan Song

songfan0026@163.com

China University of Petroleum (East China)

Yufei Liu

China University of Petroleum (East China)

Nina Su

China University of Petroleum (East China)

Zhenkui Jin

China University of Petroleum

Jing Yuan

China University of Petroleum (East China)

Article

Keywords: Sequence stratigraphy, Sedimentary system, Tertiary, Quantitative Lithofacies Paleogeography, Hydrocarbon exploration potential, Qaidam Basin

Posted Date: August 20th, 2026

DOI: https://doi.org/10.21203/rs.3.rs-10464947/v1

License: This work is licensed under a Creative Commons Attribution 4.0 International License.
Read Full License

Additional Declarations: No competing interests reported.

Sequence stratigraphy, sedimentary systems and implications for hydrocarbon exploration in the Qaidam Basin, Northern China

Fan Song [a, *], Yufei Liu [a], Nina Su [a], Zhenkui Jin [b], Jing Yuan [a]

[a] Key Laboratory of Deep Oil and Gas (China University of Petroleum (East China)), Qingdao 266580, China

[b] Key Research Laboratory of Petroleum Reservoir, China University of Petroleum, Beijing 102249, China

[*] Corresponding author.

E-mail address: songfan0026@163.com

Abstract

The Qaidam Basin is endowed with abundant Tertiary hydrocarbon resources and possesses major exploration potential. Lacking an overall understanding on sequence stratigraphy and sedimentary facies of the basin is not favorable for making new progress in hydrocarbon exploration. In this study, using outcrop, core, well logging and seismic data, the Tertiary strata of the Qaidam Basin was divided into 7 second-order sequences, 12 third-order sequences and 24 system tracts. In addition, 7 sedimentary facies types were identified, i.e., diluvial fan, braided river, flood plain, fan delta, braided river delta, lacustrine deposit and turbidite fan. Six single sedimentary factors were selected for analysis, and with third-order sequences as the unit, the distribution and evolution of sedimentary systems were defined. For the controlling factors of lithofacies paleogeography, “snow mountains controlling lakes” and “fault steps control basins” were proposed. It is believed that under a compressional tectonic setting, lake level fluctuation is closely related to elevations of peripheral mountains, and lake

water is sourced principally from mountain snowmelt. A higher structural uplifting amplitude will result in a larger area of mountain snow, a greater water supply and a larger lake area. Boundary faults of the basin retreated towards the mountains in a step way, resulting in an expanded basin. However, the faults advancing towards the center of the basin aroused basin shrinkage. From a sedimentary view, the distribution characteristics of Tertiary source rocks and reservoirs of the Qaidam Basin were analyzed; it is proposed that the periphery of the hydrocarbon generation center of the Shizigou–Mangya sag is the present-day optimum exploration zone, and the periphery of the hydrocarbon generation center of the Yiliping depression center is a potential favorable exploration zone.

Keywords: Sequence stratigraphy, Sedimentary system, Tertiary, Quantitative Lithofacies Paleogeography, Hydrocarbon exploration potential, Qaidam Basin

1. Introduction

The Qaidam Basin is one of the most significant petroliferous basins in Northern China. Within the basin, Tertiary strata exist as a major oil-bearing series. Among the 17 discovered oil fields, 15 oil fields occur in the Tertiary strata, accounting for >90% of proved petroleum reserves in the basin。The Third Resource Evaluation of China indicates that the Qaidam Basin contains hydrocarbon resources of 46.5×10^8 t equiv. and has an accumulated proved petroleum geologic reserve of 3.35×10^8 t, with a proved proportion of merely 15.6%. The basin contains a natural gas geological reserve of 3056×10^8 m^3, with a proved proportion of merely 12.2%. Therefore, the Qaidam Basin contains abundant remaining hydrocarbon resources and has a great exploration potential (Jolivet et al., 2001; Ritts et al., 2008; Zhang et al., 2020; Liu et al., 2021). Currently, obvious structure traps within the Qaidam Basin have

been discovered, targets for drilling are insufficient, hydrocarbon accumulation laws are in urgent need to study further, and favorable exploration directions need to be determined.

Distribution of source rocks and reservoirs is controlled by sedimentary facies. Precise delineation of the paleogeographic environment and sedimentary facies distribution aid in identifying the types and spatial distribution of source rocks and reservoirs, and further aid in discovering favorable directions of exploration (Zavala et al., 2016; Cai et al., 2017; Song et al., 2020). In recent years, scholars have conducted a large amount of research into the Tertiary sequence stratigraphy and sedimentary facies of the Qaidam Basin, but most of the research outcomes have concentrated on the west and the northern margins of the basin (Metivier et al., 1998; Guo et al., 2008; Wang et al., 2011; Jian et al., 2014; Yuan et al., 2015; Li et al., 2016; Zhang et al., 2018; Carrapa et al., 2019; Bush et al., 2020). Existing research findings possess the following shortcomings: (1) a uniform sequence stratigraphic framework has not been established for the whole basin, and research into the distribution of sedimentary systems across the basin is lacking. Huang et al. (2022) demonstrated systematic discrepancies in sequence stratigraphic division schemes between the western (e.g., Yingxiongling area) and eastern (Sanhu area) Qaidam Basin, primarily attributed to challenges in lateral seismic reflector correlation. Wang et al. (2021) proposed a triple-constraint methodology integrating seismic stratigraphy, biostratigraphic dating, and detrital zircon provenance analysis to resolve the diachroneity of sequence boundaries across different structural units. Liu et al. (2020) identified vertical allocyclic characteristics of "retreating western vs. prograding eastern" delta systems along the Altun and Kunlun piedmonts through paleocurrent statistical analysis. However, their study lacked basin-scale

isochronous constraints for constructing comprehensive planar facies distribution models. (2) various areas within the basin have been studied to vastly different degrees, with non-oil fields and non-hydrocarbon-bearing series being of low study degree, which is not favorable for discovering new areas and series of strata. Jolivet et al. (2018) quantified a pronounced spatial bias in outcrop distribution within the Qaidam Basin, with 85% of documented sections concentrated in the hydrocarbon-rich Yingxiongling–Western Qaidam provinces, while the eastern Delingha–Wulan region accounts for only 7%. This imbalance has forced reliance on analog-based extrapolation for reconstructing depositional models of non-reservoir strata (e.g., Lulehe Formation). Zhang et al. (2023) highlighted critical limitations in subsurface imaging along the Qilian Shan piedmont, where high-resolution 3D seismic coverage remains sparse (⩽15% of the area), severely hindering the identification of subtle traps in structurally complex zones. (3) sedimentary facies research is mostly qualitative, determination of sedimentary units lacks a quantitative basis and this determination suffers from randomness. Sun et al. (2023) highlighted that basin-wide systematic geochemical datasets (e.g., Sr-Nd isotopic compositions and clay mineral assemblages) exhibit limited coverage (<30%), significantly constraining quantitative analysis of provenance-sedimentary facies relationships. (4) the controlling factors of sedimentary distribution is not defined, which is not favorable for revealing the essence of lithofacies paleogeography evolution. Xu et al. (2020) proposed that the Late Miocene lake basin expansion was primarily controlled by the uplift of the Altun Shan (with uplift rates >1.2 mm/yr), whereas Yang et al. (2021) emphasized the dominant role of intensified Indian monsoon precipitation (evidenced by an 8‰ decrease in δD values of leaf wax biomarkers) in

driving lacustrine transgression.

The objectives of this article are to: (1) establish the Tertiary sequence stratigraphy framework for the whole Qaidam Basin and outline the developmental characteristics and spatial distribution of sedimentary systems across the basin; (2) identify the controlling factors of lithofacies paleogeography distribution and evolution and point out the spatial distribution of superior source rocks and reservoirs. This study pioneers the development of an integrated third-order sequence stratigraphic framework for the Qaidam Basin through synthesizing multi-disciplinary datasets from outcrop sections, drill cores, wireline logs, and 3D seismic volumes. The sequence stratigraphic approach proves critical in resolving basin evolution patterns, enabling precise identification of depositional system and predictive modeling of source rock distribution. Our approach not only delineates the spatiotemporal distributions of depositional facies with unprecedented resolution across discrete evolutionary stages but also establishes a novel mechanistic model delineating the interplay of tectonic-climatic drivers in controlling facies architecture evolution. The study outcomes are of great theoretical and practical significance to making new breakthroughs in hydrocarbon exploration in the Qaidam Basin.

2. Geological background

The Qaidam Basin is located in the northeast of the Tibetan Plateau in China. It is surrounded by the Kunlun Mountains, Altun Mountains and Qilian Mountains and covers an area of 12.1×10^4 km^2. The Qaidam Basin is a large Mesozoic-Cenozoic compresso-shear sedimentary basin and is principally controlled by the episodic subduction and closure of the Mesozoic and Cenozoic Tethys, as well as the remote effect from the collision of the Indian

plate with the Eurasian plate (Tian et al., 2018; Zhang et al., 2020). Since the Indo-china movement, the basin has remained in a subsidence stage and gradually transitioned from a faulted basin to a depression basin. The subsidence center continuously expanded eastward (Su et al., 2015). The basin is further divided into 4 first-order tectonic units (Western uplift, Yiliping depression, Northern uplift and Sanhu depression) and 11 second-order tectonic units (Fig. 1).

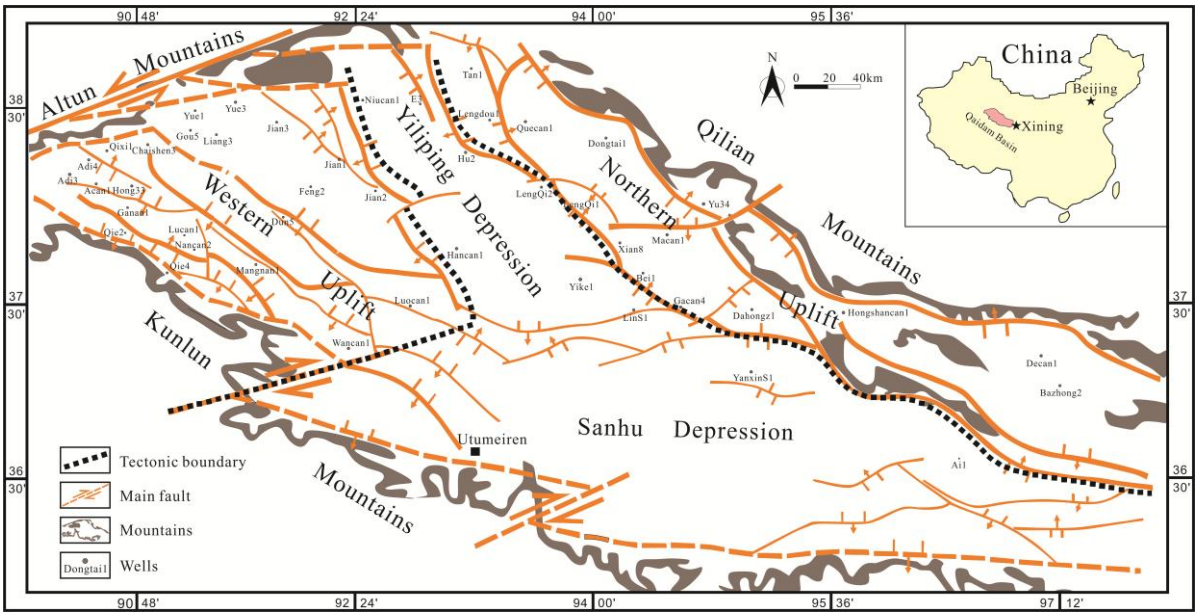


Fig.1 Division of Tertiary Tectonic Units in the Qaidam Basin, Western China.

Tertiary sediments are widely distributed within the Qaidam Basin, constituting 5000-6000 m thick clastic formation. Based on lithology, well logging, paleontology and seismic reflection characteristics, previous scholars have further divided the Tertiary sediment into seven sets of strata (Wang et al., 2008; Guo et al., 2017; Li et al., 2020). Among them, the Paleogene sediment is divided from the bottom up into the Lulehe Formation (E_{1+2}), the Lower Member of the Lower Ganchaigou Formation (E_3^1) and the Upper Member of the Lower Ganchaigou Formation (E_3^2). The Neogene sediment is divided from the bottom up into the Upper Ganchaigou Formation (N_1), the Lower Youshashan Formation (N_2^1), the

Upper Youshashan Formation (N_2^2) and the Shizigou Formation (N_2^3) (Fig. 2).

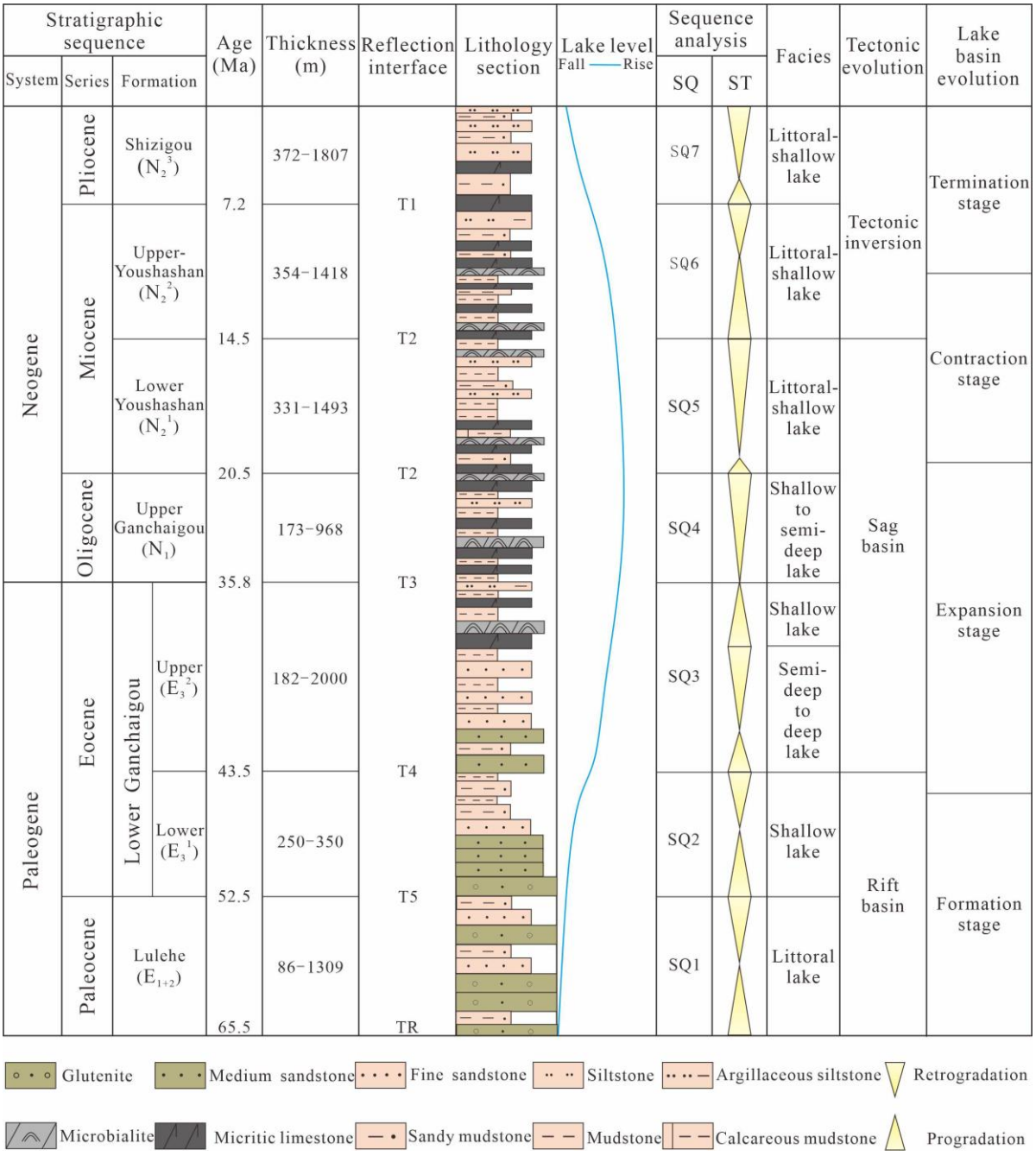


Fig.2 Composite Stratigraphic Column Showing Division and Lithofacies Associations of the Tertiary in the Qaidam Basin, Western China.

3. Datasets and methods

Tertiary stratigraphic sequences and sedimentary facies of the Qaidam Basin were investigated based on outcrop observation, core description, log data and seismic data analysis,

and experiment analysis. Well outcropped sections in the Lulehe, Jielusu, Xichagou and Lenghu areas in the Qaidam Basin were observed and more than 30 sections, totaling >10 km long, were measured. More than 500 typical wells were selected. Through multidisciplinary integration, outcrop data provided ground-truth calibration for stratigraphic contacts and facies transitions, core and well logs offered high-resolution vertical characterization of lithology and depositional features, while seismic data constrained regional architecture and lateral continuity through reflector terminations and stratal geometry interpretation. Specifically, seismic reflection patterns were calibrated with core-derived lithofacies and chronostratigraphic markers to validate lateral sequence boundaries, while discrepancies in seismic interpretations (e.g., ambiguous unconformities) were resolved by direct lithological evidence from cores, achieving iterative refinement between subsurface imaging and in-situ stratigraphic records. Using well logging and core data, single-well sequences, systems tracts and parasequences were divided. By applying 25 regional seismic sections and 3D seismic data within the basin, a seismic sequence division was conducted. Finally, by comprehensively analyzing outcrops, drilling wells and seismic sequences, sequences and system tracts were divided, and the Tertiary sequence stratigraphic framework was established for the whole basin.

Llithologies, mudstone color, paleontology and trace elements were comprehensive analyzed through core and cutting data of 80 wells, and the Tertiary sedimentary environment of the Qaidam Basin was determined, including paleoclimate, paleosalinity and paleo-water-depth. Accordingly, recognition indicators for sedimentary facies were established through a comprehensive study of outcrops, lithofacies, logging facies and seismic

facies, and the Tertiary sedimentary facies types of the Qaidam Basin were determined. With third-order sequences as the mapping unit, and using the "single-factor analysis and multi-factor mapping method", the Tertiary lithofacies paleogeographic map of the whole basin was compiled to analyze the distribution characteristics and evolution history of sedimentary systems. During the mapping process, individual maps including stratigraphic thickness, sandstone thickness, conglomerate thickness, sandy conglomerate percentage, dark mudstone content, and carbonate rock content, were made to clarify the quantitative distribution characteristics of each single factor. These analyses were subsequently integrated into a unified paleogeographic map through systematic synthesis of their spatial relationships, overlaps, and interactions. From the perspective of paleoclimate and basin evolution, the controlling factors of lithofacies paleogeography evolution were comprehensively analyzed. The data herein was provided by the Research Institute of Petroleum Exploration & Development, Qinghai Oilfield Company, PetroChina. All research work and experiments were conducted in the State Key Laboratory of Petroleum Resource and Prospecting of the China University of Petroleum.

4. Results

4.1 Sequence stratigraphic framework

4.1.1 Sequence boundaries

Sequence boundaries were recognized using outcrops, drilling, logging and seismic data to divide sequence units. Well outcropped sections in the Lulehe, Jielusu, Xichagou and Lenghu areas were observed in detail. Unconformities, and regional discontinuity surfaces of lithology and lithofacies were identified as sequence boundaries by considering such factors

as the stratigraphic contact relationship, vertical variation of color and lithology, piling style and river erosion. The easily recognized sequence boundaries in field outcrops mainly include the Paleogene/Cretaceous, Lower Youshashan Formation/Upper Ganchaigou Formation, and Upper/Lower Ganchaigou Formations interfaces (Fig. 3).

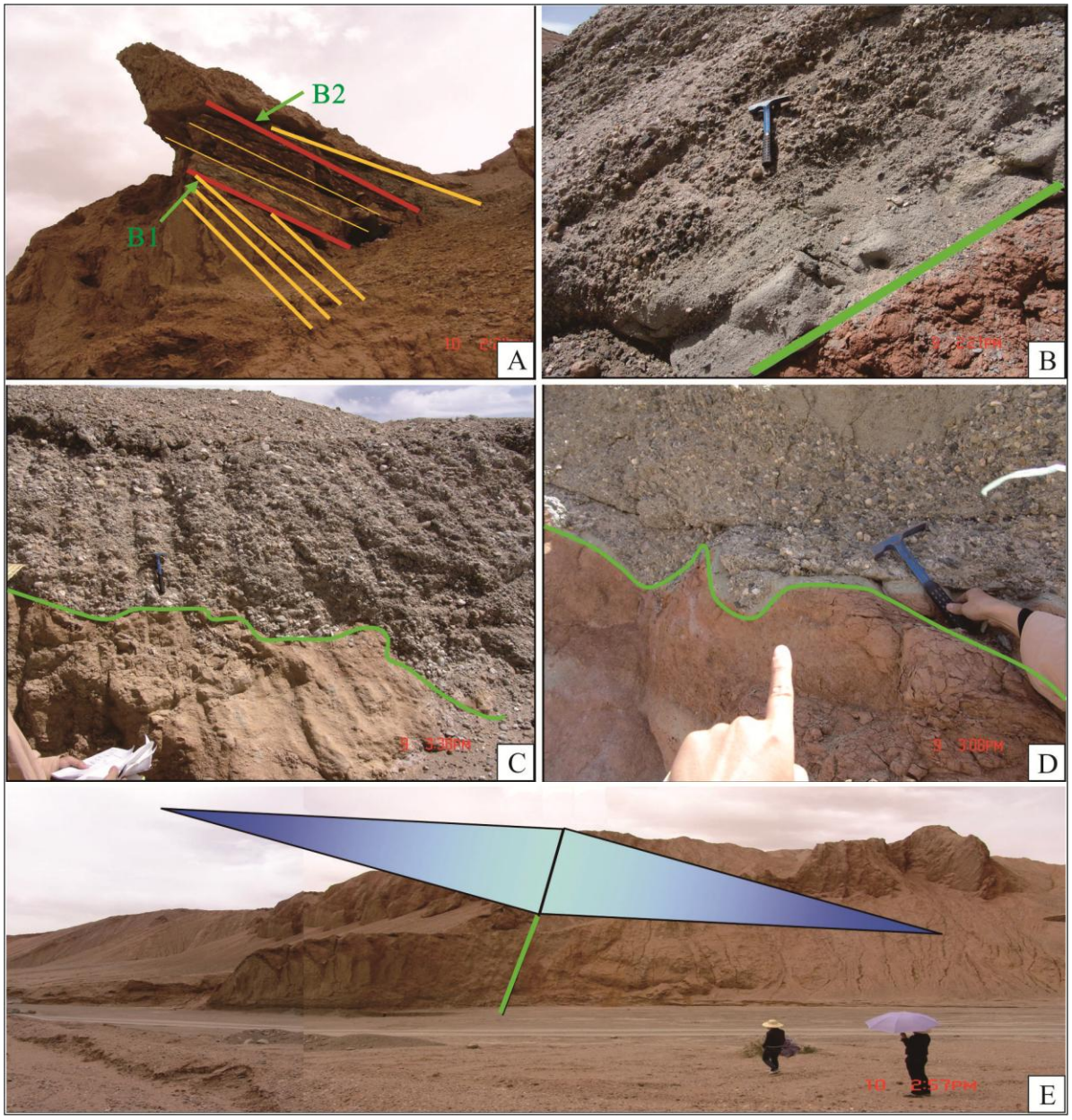
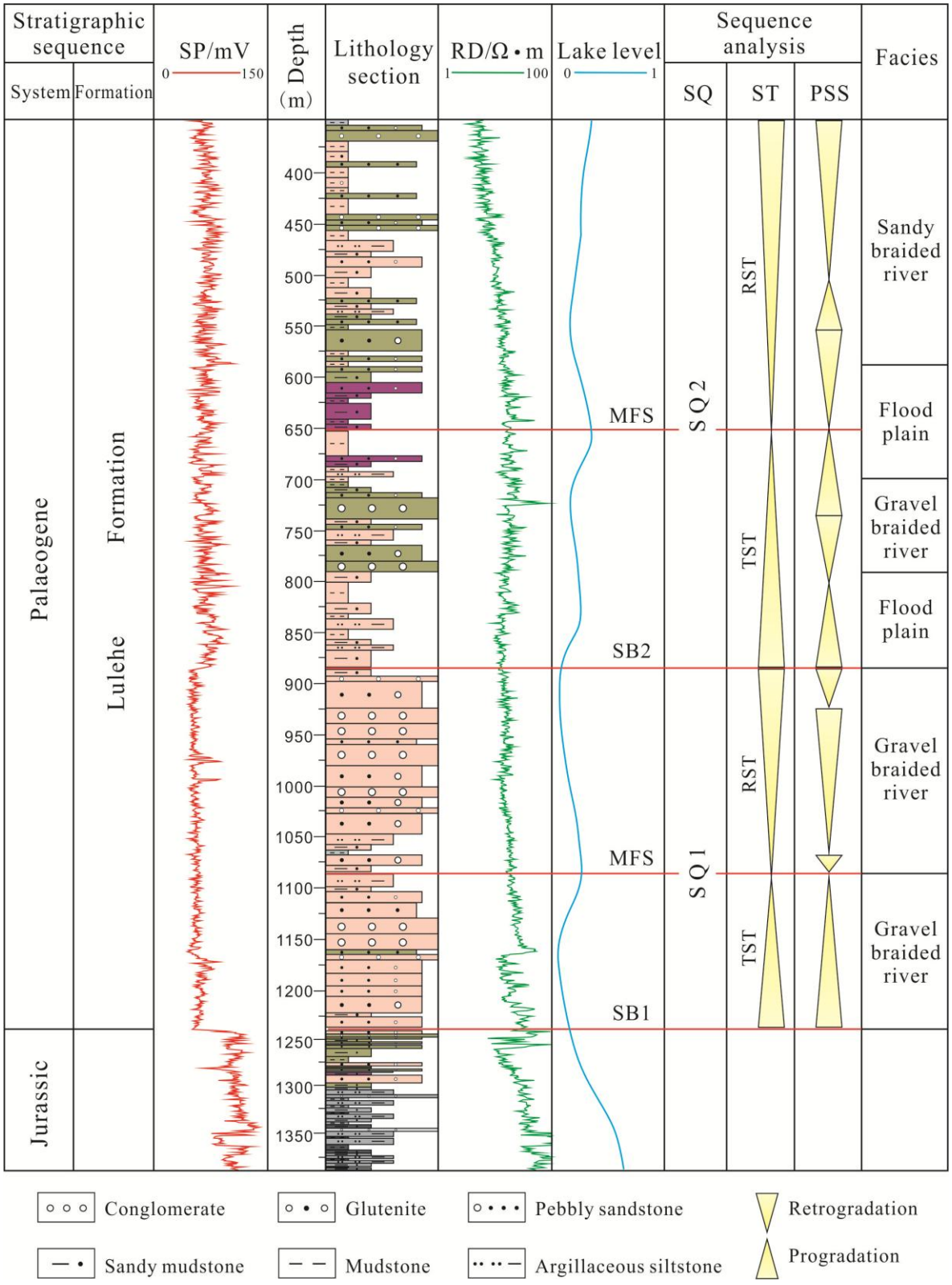


Fig.3 Sequence boundary identification mark from outcrop section in the Qaidam Basin. (A) Angular unconformity. B1 is the boundary between Jurassic and Cretaceous, B2 is the boundary between Cretaceous and Paleogene. From Jielusu section. (B) The bottom of Lower

Youshashan Formation. From Lulehe section. (C) The bottom of Lower Ganchaigou Formation. From Lenghu section. (D) The bottom of Lower Ganchaigou Formation. From Lenghu section. (E) The boundary between Upper/Lower Ganchaigou Formations. From Jielusu section.

As sedimentation differs above and below a sequence interface, lithofacies also differ, forming a lithofacies transitional surface easily recognized by drilling and logging. Analysis of the previously mentioned 500 wells within the basin indicates that on transitional surfaces of lithofacies, natural potential and resistivity log curves are in discontinuity (Fig. 4). About 25 regional seismic sections across the basin were applied to recognize unconformities and other sequence interfaces according to seismic reflection characteristics. Seismic sequences and seismic facies were divided, and eight seismic reflection layers with distinct characteristics, i.e., T_0, T_1, T_2', T_2, T_3, T_4, T_5 and T_R, were recognized (Fig. 5A-B). These reflection layers correspond respectively to the top and bottom interfaces of the seven Tertiary sets of strata within the Qaidam Basin and are second-order sequence interfaces. By synthesizing the geological and geophysical response characteristics of sequence boundaries, the Paleogene–Neogene of the Qaidam Basin is divided into six second-order sequences and 12 third-order sequences (Table 1). While aligning with Vail's hierarchy in cyclicity ranking (1-3 Myr duration), the third-order sequences in this study are tectonically driven by Altyn Tagh fault pulses, exhibiting abrupt thickness variations across syndepositional faults rather than eustatic controls characteristic of marine basins.

208



209

210 Fig.4 Characteristics of lithology and well-log responses at sequence boundaries in the

211 Paleogene Lulehe Formation of Qaidam Basin. (SQ-sequence; ST-systems tract;

PSS-parasequence set).

Table 1

Sequence stratigraphic division chart of the Tertiary in the Qaidam Basin: showing the classification of Paleogene-Neogene Formations and their corresponding Sequences and System Tracts.

Stratigraphy			Sequence				Seismic reflection layer
System	Series	Formation	First-order	Second-order	Third-order	Systems tract	
Quaternary	Pleistocene	Qigequan					
							T_0
Neogene	Pliocene	Shizigou (N_2^3)	II	VII	SQ12	RST	
						TST	T_1
	Miocene	Upper Youshashan (N_2^2)		VI	SQ11	RST	
						TST	T_2'
		Lower Youshashan (N_2^1)		V	SQ10	RST	
						TST	
					SQ9	RST	
						TST	T_2
	Oligocene	Upper Ganchaigou (N_1)		IV	SQ8	RST	
						TST	
					SQ7	RST	
						TST	T_3
Paleogene	Eocene	Lower Ganchaigou Upper (E_3^2)	I	III	SQ6	RST	
						TST	
					SQ5	RST	
						TST	T_4
		Lower Ganchaigou Lower (E_3^1)		II	SQ4	RST	
						TST	
					SQ3	RST	
						TST	T_5
	Paleocene	Lulehe (E_{1+2})		I	SQ2	RST	
						TST	
					SQ1	RST	
						TST	
							TR

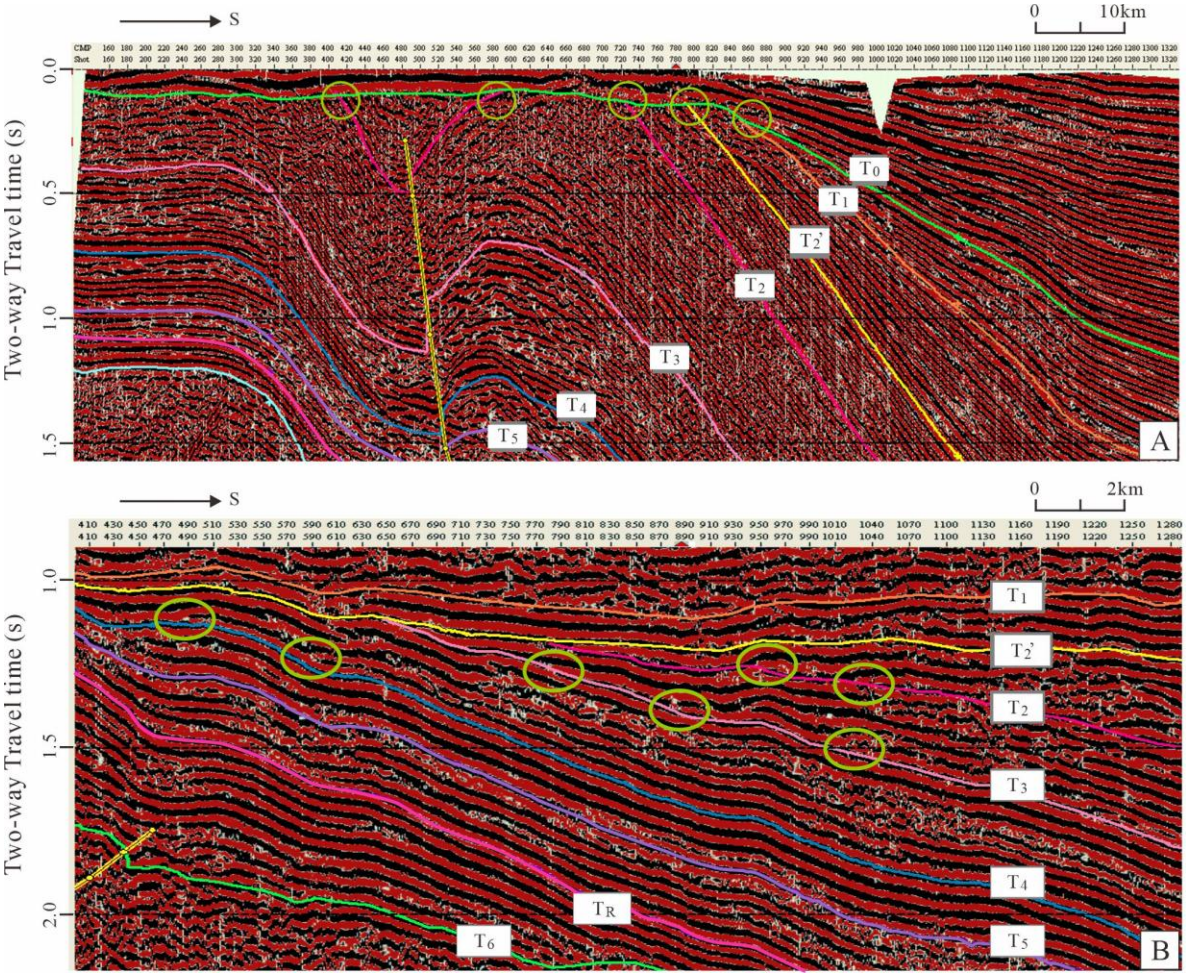


Fig.5 Seismic section (north to south) across the Qaidam Basin showing the sequence boundaries and stratigraphic units. (A) Truncation reflection characteristics (Line cdm 1150). (B) Onlap reflection characteristics (Line 831050).

4.1.2 Stacking patterns of system tracts

In research of continental facies lacustrine-basin sequence stratigraphy, first flooding surface (FFS) and maximum flooding surface (MFS) are typically used to divide systems tracts (Jiang et al., 2011; Song et al., 2018; Zhang et al., 2019). As slope break zones are rare along the margin of the Qaidam Basin (Su et al., 2014), transgressive systems tracts (TST) and regressive systems tracts (RST) are divided in this study, and their interface is determined

mainly based on MFS (Table. 1). The seismic reflections of the MFS are not well defined, but they are marked in log patterns due to the abrupt changes in lithology (Fig. 6). The MFS in the western basin is chiefly composed of dark mudstone and oil shale, and the northern margin and the east of the basin are mainly brownish red and grayish green mudstone. With the MFS as the boundary, the internal para-sequence stacking style varies vertically from retrogradation to progradation from the TST to the RST (Fig. 6).

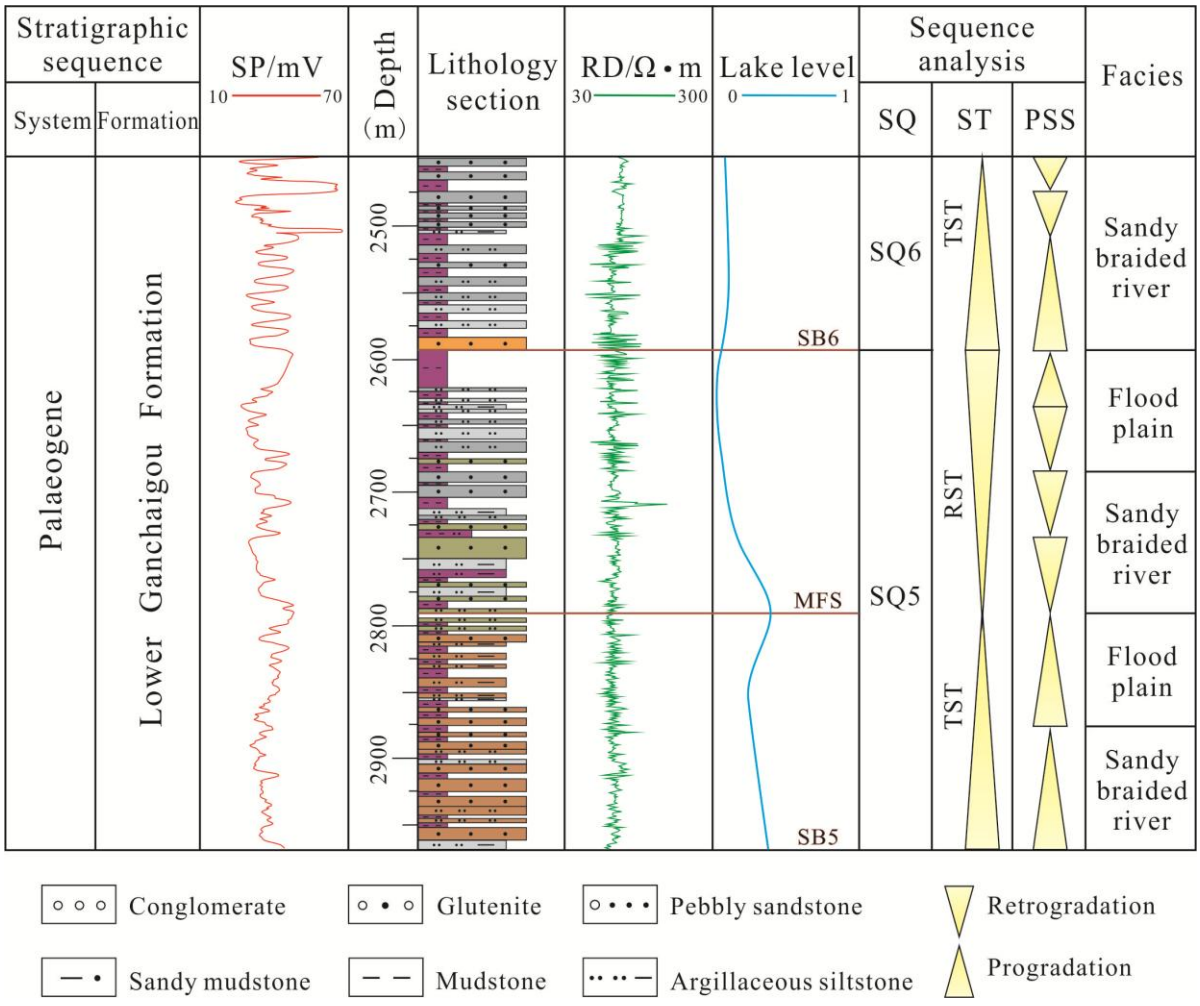


Fig.6 Characteristics of lithology and well-log responses at sequence boundaries in the Paleogene Lower Ganchaigou Formation of Qaidam Basin. (SQ-sequence; ST-systems tract; PSS-parasequence set).

4.2 Sedimentary characteristics

4.2.1 Lithology

The Qaidam Basin contains a variety of rock types, which mainly includes clastic rocks, carbonate rocks, gypsum and salt rocks (Table 2). Among them, clastic rocks are the most dominant rock type within the basin and are widely distributed in various horizons of the Tertiary strata. They are dominated by conglomerate, sandstone, siltstone and mudstone. Within the Qaidam Basin, the climate is dry, the Tertiary lake basin is dominated by a half-saline to saline water environment (Hu et al., 2012; Song et al., 2018), and lake water has high salinity, favoring deposition of carbonate rocks, gypsum and salt rocks. Carbonate rock types are variety within the basin, and mainly include marlstone, algal limestone and grainstone. They are chiefly distributed in the Upper Member of the Lower Ganchaigou Formation (SQ5-SQ6), the Upper Ganchaigou Formation (SQ7-SQ8) and the Lower Youshashan Formation (SQ9-SQ10). The proportion of carbonate rocks is comparatively high in the Upper Member of the Lower Ganchaigou Formation. According to the statistics of core and log data, gypsum mainly exists in the Shizigou, Hongliuquan and Nanyishan areas and is present vertically in the Upper Ganchaigou Formation (SQ7-SQ8). The quantity of gypsum is comparatively low and only minor salt rocks associated with mudstone are found in the Shizigou area.

4.2.2 Sediment grain size

The grain-size analysis of 80 core samples suggests that the grain-size accumulation probability curves mainly has three sub-populations, namely rolling, saltation, and suspended sub-populations, and they generally reflect tractive current-dominated sedimentation characteristics. The grain-size accumulation probability curve of gravelly braided river

channels within the basin is mainly three-segmented, and that of sandy braided rivers is

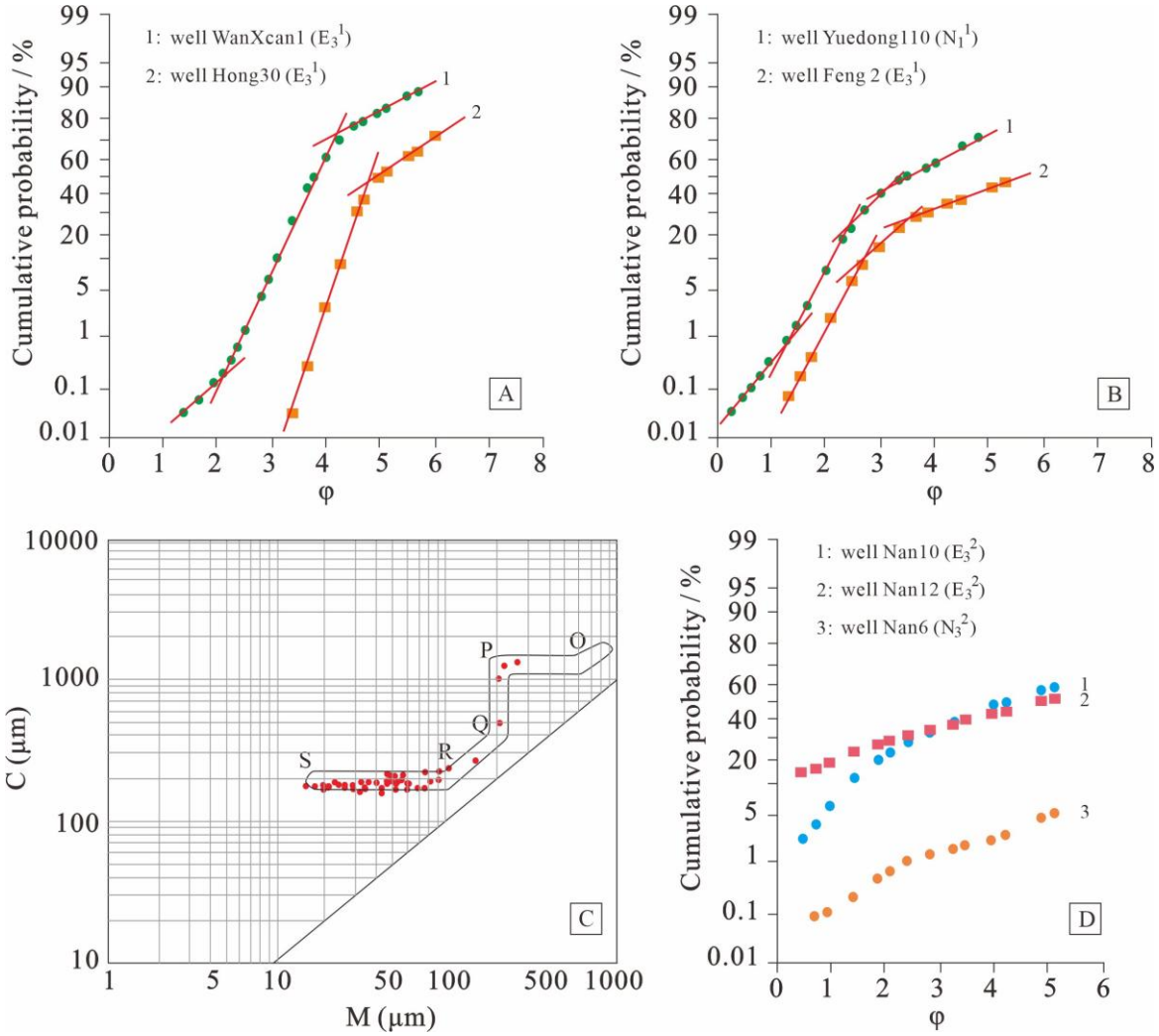
Table 2

Rock types and characteristics of the Tertiary strata in the Qaidam Basin.

Rock types			Grain size /mm	Sedimentary facies
Clastic rocks	Conglomerate	Coarse	>100	Diluvial fan
		Medium	10～100	Diluvial fan, Gravel braided river
		Fine	2～10	Diluvial fan, Gravel braided river, Sandy braided river
	Sandstone	Coarse	0.5～2	Diluvial fan, Gravel braided river, Sandy braided river
		Medium	0.25～0.5	Gravel braided river, Sandy braided river
		Fine	0.1～0.25	Delta, Sandy braided river, shore–shallow lake
	Siltstone		0.01～0.1	Sandy braided river, Flood plain, shallow lake, Semi-deep lake
	Mudstone	Brownish red	<0.01	Flood plain
		Dark grey		Lake, Delta
Carbonate rocks	Limestone	Argillaceous limestone		Semi-deep lake, Deep lake
		Algal limestone		Lime-mud flats in shallow lake
		Grainstone		Grain beach in shallow lake
Evaporite	Gypsum rock			Semi-deep lake, Deep lake
	Salt rock			Semi-deep lake, Deep lake

mainly two-segmented, lacking rolling sub-populations (Fig. 7A). There are two types of grain-size accumulation probability curves of front-delta underwater distributary channels. The first is three-segmented, as represented by underwater distributary channels formed in a comparatively stable water period, and the second is compound, as represented by underwater distributary river channels formed in a flooding period (Fig. 7B). The C-M diagram is mainly constituted by RS segments (which represent poorly sorted deposits dominated by rolling/saltation transport) and QR segments (which reflect well-sorted sedimentation under

271 homogeneous suspension), both indicating even homogeneous suspension and graded
272 suspension transportation characteristics and reflecting a tractive current flow mechanism (Fig.
273 7C). In addition, there are minor turbidity sediments, whose grain-size accumulation
274 probability curve is a low-slope straight line segment or a broad, gently-dipping
275 arching-upward curve segment. The grain-size intervals span widely, and jumping and rolling
276 are generally not developed (Fig. 7D).



277

278 Fig.7 Sediment grain size analysis diagram of the Tertiary in the Qaidam Basin. (A) Braided
279 river channel. (B) Underwater distributary channel of delta front. (C) C-M diagram. O:
280 Deposits in specific fields, rarely labeled in standard C-M plots; P: Highest C and M values,
281 represent graded suspension; Q: Shift from graded to uniform suspension; R: Transition to

282 rolling/saltation; S: Lowest C and M, represent pure rolling. (D) Grain size probability curve
283 of braided channel of sublacustrine fan.

284 *4.2.3 Sedimentary structures*

285 Field outcrop and core observation implies that a variety of Tertiary bedding types are
286 developed in the Qaidam Basin, mainly including horizontal bedding (Fig. 8A), parallel
287 bedding, cross bedding, graded bedding, massive bedding, lenticular bedding and wavy
288 bedding. Of them, parallel bedding and various cross bedding are the most common and
289 widely distributed in fluvial facies, fan delta, delta, shore–shallow lacustrine facies and
290 sublacustrine fan (Fig. 8B–8D). Lenticular bedding and wavy bedding are formed in an
291 environment of alternated strong and weak hydrodynamic forces, mostly observable in
292 siltstone and silty mudstone and mainly developed in flood plains in the Qaidam Basin.

293 Some bedding-plane structures and biogenetic structures are observable within the area.
294 Bedding-plane structures are mainly ripple marks, which exist on bedded surfaces of sandy
295 sediments and include current ripple marks and wave-formed ripple marks. Of them, current
296 ripple marks indicate water flow directions and wave-formed ripple marks represent shallow
297 water sedimentary environments (Fig. 8E). Biogenetic structures mainly include bioglyph,
298 bioturbation structures and plant root and stem structures. Bioglyph is mainly observable in
299 fine sandstone and siltstone, and generally perpendicular or oblique to bedded planes.
300 Bioturbation structures include superficial and intrabed bioturbation; the former usually
301 occurs in low-energy sedimentary environments and the latter reflects high energy
302 environments (Fig. 8F). The Tertiary strata in the western basin preserves a small amount of
303 paleo-plant root traces, which are mainly distributed in the Upper Member of the Lower

Ganchaigou Formation and the Lower Youshashan Formation and mostly preserved as charcoal debris.

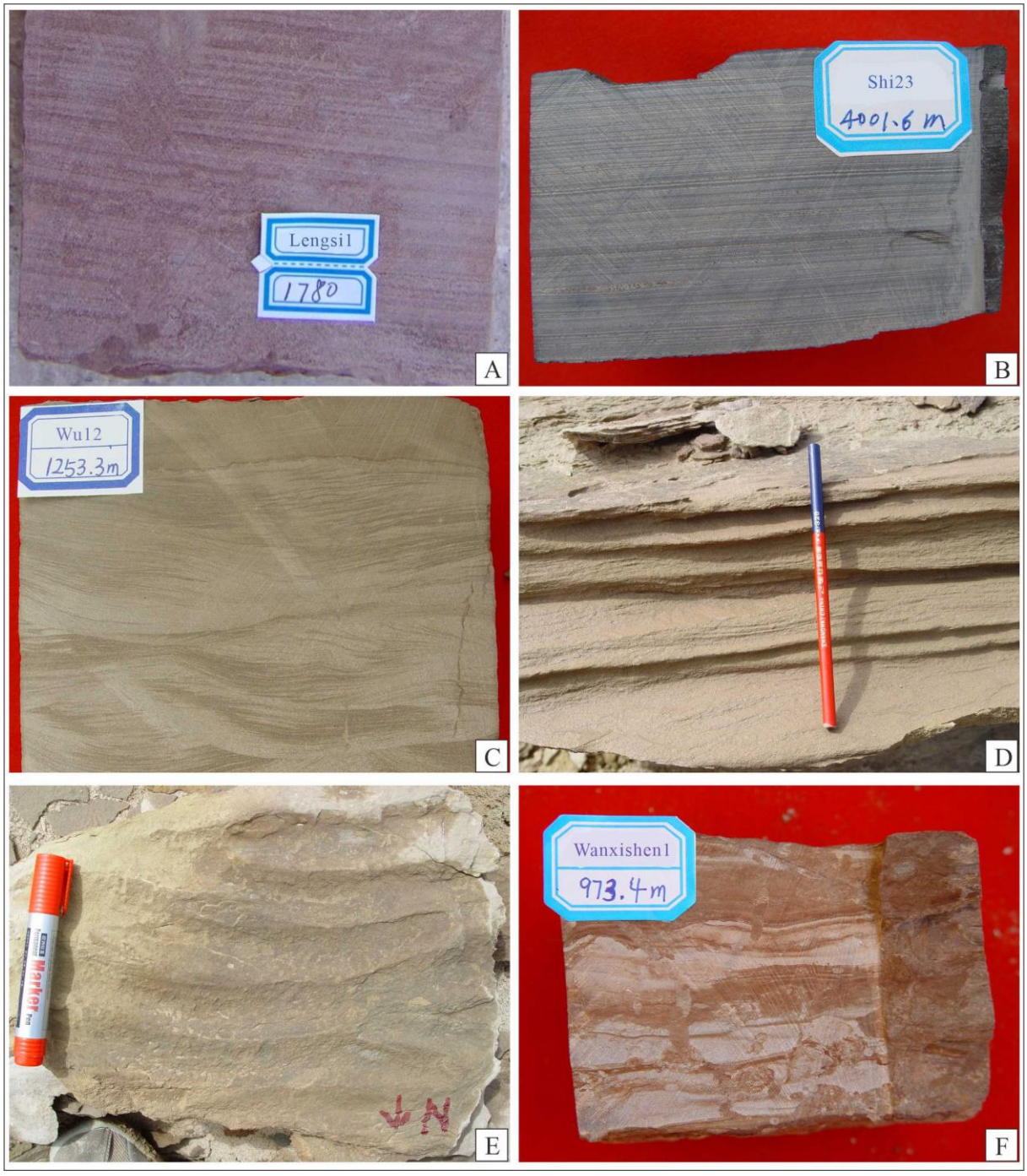


Fig.8 Sedimentary structures of the typical sedimentary facies in the Qaidam Basin. (A) Horizontal bedding. From Well Lengsi1 at 1780m. (B) Parallel bedding. From Well Shi23 at 4001.6m. (C) Trough cross-bedding. From Well Wu12 at 1253.3m. (D) Swash cross-bedding.

From Lenghu section. (E) Wave-formed ripple marks. From Xichagou section. (F) Bioturbation structures. From Well Wanxishen1 at 973.4m.

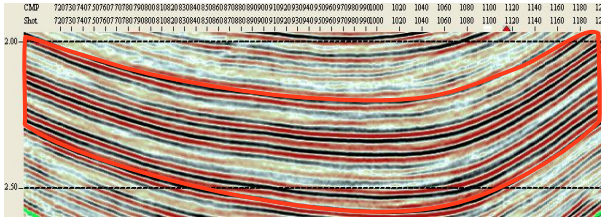
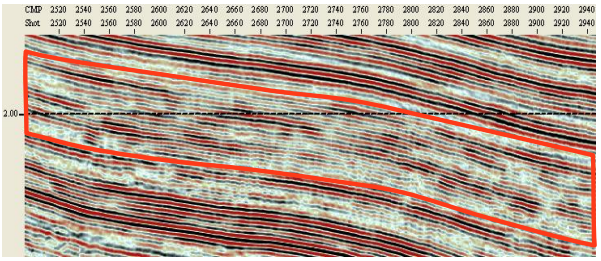
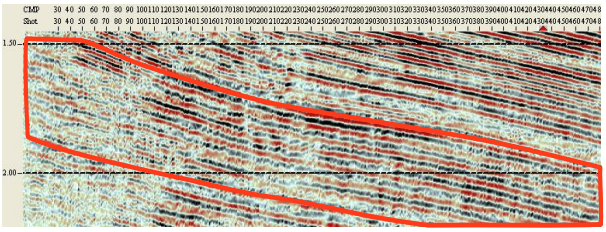
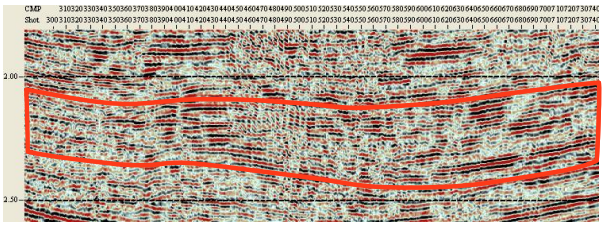
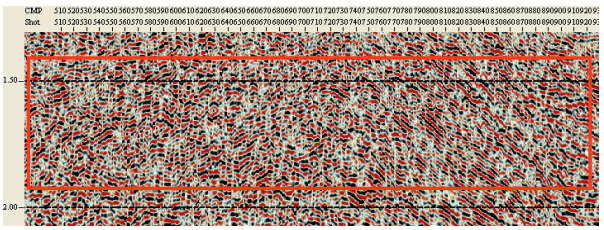
4.2.4 Geophysical characteristics

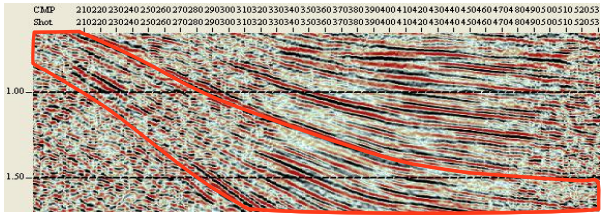
Well logging curve shapes of the study area include bell-shaped, box-shaped, combined bell–box shaped and funnel shaped and represent different sedimentation types. Bell-shaped curves are widespread within the area, mostly with micro-zigzags. The curves usually have abrupt contact on the bottoms, with amplitude decreasing gradually upwards, and represent typical delta and river channel deposits. In addition, box-shaped curves are common within the area and of middle amplitude; they have bottoms and tops both in abrupt contact, and usually represent thick-bedded, massive sedimentary bodies of fluvial fan and braided river facies. The lower intervals of combined bell–box shaped curves are dominated by conglomerate and pebbled sandstone, gradually transitioning upwards into fine sandstone and siltstone, and represent positive rhythmic sedimentation signatures of river channels. Funnel-shaped curves are rare within the area. They are of low amplitude, observable in delta estuary bars, and mainly composed of fine sandstone and siltstone, gradually fining from lower upwards. High-quality seismic sections that cover the area were selected for seismic facies research, and the internal reflection structure, outer geometrical morphology, reflection continuity, reflection amplitude, reflection frequency and interval velocity of the seismic sections were comprehensively analyzed. Six variable seismic facies types were identified, including parallel high continuous reflection facies, subparallel high continuous reflection facies, wavy progradational reflection facies, progradational fill reflection facies, clutter reflection facies, and wedge-shaped onlap reflection facies, and their characteristics are shown

in Table 3. Determination of these seismic facies types provides basis for the sedimentary facies division of areas with sparse wells and lack of outcrops and cores within the basin.

Table 3

Seismic section patterns and reflection characteristics of depositional facies types in the Tertiary of the Qaidam Basin.

Type	Seismic section	Characteristics
Semi-deep lake		High frequency, medium–strong amplitude, high continuous, parallel sheet reflection, represents a typical low-energy environment.
Shallow lake		Medium–high frequency, Medium–weak amplitude, high continuous, subparallel reflection, the seismic event is often bent, mostly distributed in the lake.
Lakeshore		Medium–high frequency, Medium–weak amplitude, medium continuous, wave reflection, commonly found in areas with relatively shallow water at the edge of lake basins.
Flood plain		Medium–low frequency, Medium–weak amplitude, medium continuous, usually shown that two continuous events in the lateral direction are separated by a set of disorderly reflected events.
Diluvial fan		Clutter reflection, represents turbulent hydrodynamic conditions.

Fan delta		Medium frequency, Medium–weak amplitude, high continuous, wedge reflection, seismic events from clutter reflection transition to high continuity, commonly found in the basin margin.

4.3 Sedimentary systems

Many types of sedimentary systems may develop in the sedimentary filling process of a faulted basin, and their distributions in different structural belts may be complicated (Gawthorpe et al., 2000; Lin et al., 2004; Song et al., 2014; Wu et al., 2015). The Tertiary sedimentary facies of the Qaidam Basin were divided into seven types according to field outcrop sections, drilling sections, core observation, well logging and seismic facies indicators, in combination with the regional distribution patterns of different lithology. These types include diluvial fan, braided river, flood plain, fan delta, braided river delta, lake and turbidite fan (Table 4).

Table 4

Sedimentary facies type and the main distribution area of the Tertiary Formation in the Qaidam Basin.

Facies	Subfacies	Microfacies	Distribution
Diluvial fan	Upper fan	Main channel, gravelly floodplain	The piedmont of Altun Mountains, Kunlun Mountains, and Qilian Mountains
	Middle fan	Braided channel, sandy floodplain	
	Outer fan	Channel, sandy floodplain	
	Between fans	Argillaceous floodplain	
Braided river	River channel	Main channel, branch channel	The piedmont of Altun Mountains, Kunlun Mountains, and Qilian Mountains
	Overbank	/	
Flood plain	/	/	Widely distributed in the Basin
Fan delta	Fan delta plain	Distributary channel, interdistributary bay	Qigequan area, Xianshuiquan area, and Hongliuquan area
	Fan delta front	Subaqueous distributary channel, estuary bar, sheet sand	
	Pro-fan delta	Lacustrine mudstone	
Braided	Delta plain	Branch channel	Dafengshan area, Eboliang area,

river delta	Delta front	Subaqueous distributary channel, estuary bar, distal bar	and Yuejin area
	Pro-delta	Lacustrine mudstone	
Lacustrine deposit	Shore shallow lake	Beach bar, lacustrine mudstone	Widely distributed in the Basin
	Semi-deep lake	Lacustrine mudstone, turbidite	Shizigou area, Yingxiongling area, Mangya–Yiliping area
Turbidite fan	Upper fan, middle fan, outer fan	Gravity flow channel	Steep slope in the margin of the lacustrine basin

4.3.1 Diluvial fan

Diluvial fans are chiefly distributed in the piedmont zones of the Altun Mountains, Qilian Mountains and Kunlun Mountains and longitudinally developed in the Lulehe Formation, the Lower Member of the Lower Ganchaigou Formation and the Upper Ganchaigou Formation. Diluvial fan sediments are coarse-grained and lithologically dominated by reddish brown conglomerate and glutenite, followed by sandstone, siltstone and minor mudstone. In cross sections, the proportion of glutenite is generally above 50%, and the argillaceous matrix is usually brownish red and purple red. Conglomerates have low maturity in composition and structure and are poorly sorted and rounded, with pebbles in disordered accumulation (Fig. 9A).

4.3.2 Braided river and flood plain

Braided rivers are contiguously distributed in peripheral piedmont zones of the basin, and river channels show distinct downcutting, with scouring planes in abrupt contact with the underlying strata. Rock types mainly include sandstone, glutenite and minor mudstone. Glutenite accounts for more than 20% and clastic grains are fining upwards. River channel sands are well continuous laterally, in which parallel bedding, tabular cross-bedding and wedge cross-bedding are usually developed (Fig. 9B–9D). The Qaidam Basin possessed a dry climate during the Paleogene (Hu et al., 2012), and large-scale flood plains were developed outside river channel sediments. Flood plains are flat in terrain with rare river channels and

are exposed to a strong oxidation environment for a long time. The sediments are dominated by red, brownish mudstone and argillaceous siltstone, with weak horizontal bedding, and are mostly massive. Flood plains are widespread within the basin; thus, they are considered as a separate type of sedimentary facies.

4.3.3 Fan delta

In Paleogene, fan deltas are chiefly distributed in the steep slope of the piedmont of the Altun Mountains. They are dominated by coarse sandstone and glutenite of underwater distributary river channel facies, with parallel and small-sized cross bedding developed. In Neogene, fan deltas are chiefly distributed in the Upper Ganchaigou and Lower Youshashan Formations. In plan view, they are mainly distributed in comparatively steep slope areas like Xianshuiquan, Ganchaigou and Jiandingshan in the piedmont of the Altun Mountains, and the Qiekelike area in the piedmont of the Kunlun Mountains. Fan delta plains and front sub-facies can be recognized in Neogene fan deltas. Sediments are dominated by coarse clasts, mostly conglomerate and glutenite interbedded with thin siltstone and fine sandstone (Fig. 9E).

4.3.4 Braided river delta

Braided river deltas are widely distributed in the Alaer, Dafengshan and Yuejin areas of the western basin and Niubiziliang, Lulehe and Lenghu areas in the northern basin. They are mainly distributed in the Lower Ganchaigou Formation, the Upper Ganchaigou Formation and the Lower Youshashan Formation. According to sedimentary characteristics, braided river delta plain and front sub-facies were recognized. Of these, the braided river delta plain mainly comprises glutenite and oxidative mudstone of above water sedimentary origin, and the braided river delta fronts mainly comprise sandstone, siltstone and grayish green mudstone.

The sediments are generally well sorted and rounded. Cross bedding and parallel bedding are common in sandstone.

4.3.5 Lacustrine deposit

The Tertiary strata of the Qaidam Basin is dominated by shore–shallow lake and semi-deep lake subfacies, without deep lake facies. Shore–shallow lake facies occur in weak oxidation–reduction environments and are dominated by dark mudstone, siltstone and fine sandstone. They usually have bimodal cross-bedding, lenticular bedding, ripple mark and bioturbation structures (Fig. 9F–9H). Semi-deep lake facies are located in weak reduction environments and are dominated by dark mudstone with horizontal bedding (Fig. 9I).

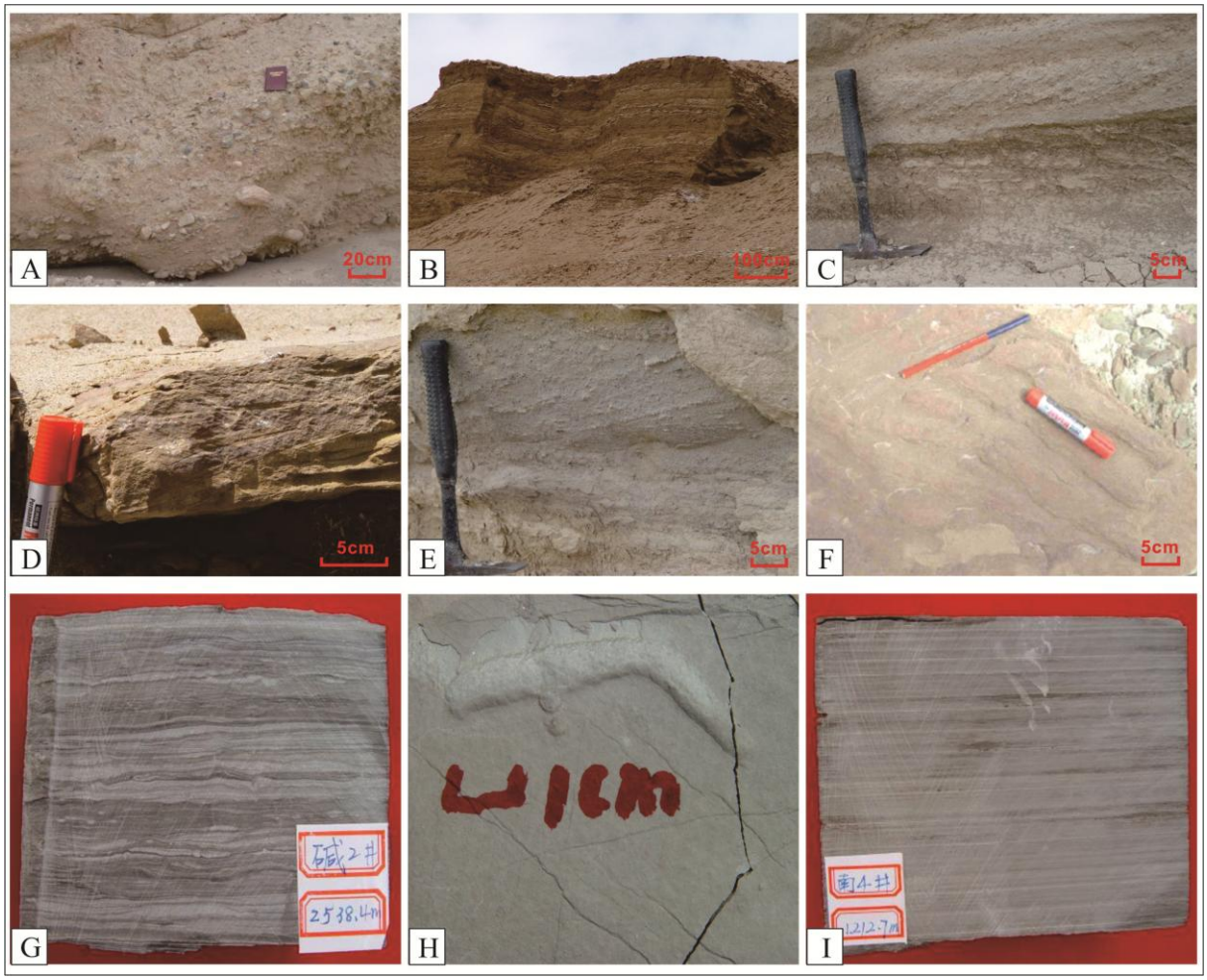


Fig. 9 Typical sedimentary phenomenon of the main sedimentary facies in the Qaidam Basin.

(A) Conglomerate of diluvial fan. From Lenghu section, N_2^1. (B) Parallel bedding. From Youshashan section, N_2^2. (C) Pebbled coarse sandstone with tabular cross-bedding. From Xichagou section, N_1. (D) Wedge cross-bedding. From Dongchaishan section, N_1. (E) Pebbled coarse sandstone of fan delta. From Xichagou section, E_3^2. (F) Ripple mark in fine sandstone of shore lake facies. From Dongchaishan section, E_3^1. (G) Lenticular bedding. From Well Jian2 at 2538.4m. (H) Bioturbation structures in mudstone. From Xichagou section, N_1. (I) Horizontal bedding. From Well Nan4 at 1212.7m.

4.3.6 Turbidite fan

Turbidite fans are fan-shaped clastic rock bodies of deep water gravity origin and are formed by slumping and re-deposition of alluvial fans–fan deltas. Turbidite fans are comparatively rare within the study area. They are principally distributed in the Upper Member of the Lower Ganchaigou Formation along Huatugou and Xianshuiquan in the piedmont of the Altun Mountains and characterized by sandstone and conglomerate intercalated with gray mudstone and marl. The lithologies are poorly sorted and variable in size; incomplete Bouma sequences and graded bedding are common.

4.4 Distribution and evolution of sedimentary facies

Taking third-order sequences as the study unit and using the quantitative lithofacies paleogeography research method proposed by Professor Feng (Feng., 1992, 2004), i.e., the single-factor analysis and multi-factor comprehensive mapping method, sedimentary factors include strata thickness, sandstone thickness, conglomerate thickness, glutenite content, dark mudstone content and carbonate content were selected to draw the quantitative Tertiary sedimentary facies maps of the Qaidam Basin. The distribution characteristics and evolution

of sedimentary facies in the third-order sequences were summarized.

4.4.1 SQ1-SQ2

The initial period of depression of the Qaidam Basin is the depositional period of the Lulehe Formation (SQ1). During this period, with the Tibetan Plateau being gradually uplifted, subsidence occurred comparatively quickly in the piedmont zones of the Altun and Kunlun Mountains in the western basin. The Youshashan area was the subsidence center, where semi-deep lake subfacies were developed. According to seismic facies and stratigraphic thickness, it is inferred that the Hancan 1 Well Block is also a subsidence center, in which semi-deep lake subfacies were developed. Shore–shallow lake subfacies were widely developed in the Shizigou, Ganchaigou, Xianshuiquan and Yiliping areas in the periphery of semi-deep lakes. Due to the steep terrain slope in the Ganchaigou and Xianshuiquan areas, alluvial fans extended into lakes, forming fan delta sediments; the lithologies mainly include interbeds of brownish yellow conglomerate and dark mudstone. Braided rivers in the Alaer area in the piedmont of the Kunlun Mountains flowed into lakes, forming small-scale braided river delta deposits. Contiguous braided rivers were developed in the Qiekelike area. Diluvial fan deposits were mainly developed in the Yueyashan, Jiandingshan, Niubiziliang and Eboliang areas in the piedmont of the Altun Mountains, as well as in the Lukehe, Qianshan and Dongtai 1, Gaxi 1 and Yuanqiu 1 well blocks along the northern margin. Braided rivers were widely developed as contiguous zones in diluvial fan fronts. The eastern area underwent onlapping wedging-out during the period and did not receive deposits. In other areas of the basin, flood-plain red clastic deposits were widely developed (Fig. 10A).

In the depositional period of the upper part of the Lulehe Formation (SQ2), the

Youshashan and Yiliping areas remained the sedimentation–subsidence center, with semi-deep lake subfacies developing. The shore–shallow lake area in the SQ2 period expanded relative to in the SQ1 period; the shore–shallow lake in the piedmont of the Altun Mountains expanded to the Jianding Mountains, Dafeng Mountains and Dun 5 Well Block, and the shore–shallow lake in the Yiliping area expanded as well. Diluvial fans were developed in the Yueya Mountains and Niubizi Ridge in the piedmont of the Altun Mountains. Fan deltas were developed in the Xianshuiquan area. As the shore–shallow lake area expanded, the braided river in the Jianding Mountains directly flowed into the lake, forming braided river delta deposits. Compared to SQ1, braided river deltas in the Alaer disappeared, and the braided river directly transitioned into a flood plain during this period. Braided rivers were still developed in the Qiekelike area. Diluvial fans were developed in the piedmont of the Qilian Mountains along the northern margin and chiefly distributed in the Dongtai 1, Gaixi 1 and Yuanqiu 1 Well Blocks. Braided rivers widely occurred as contiguous bands in the Lenghu and Mahai areas in the fronts of alluvial fans. Distribution of sedimentary facies in other areas is basically consistent with that of the period of SQ1 (Fig. 10B).

4.4.2 SQ3-SQ4

During the depositional period of the Lower Member of the Lower Ganchaigou Formation (SQ3), lake facies deposits were developed in the western segment of the piedmont of the Altun Mountains and Yiliping area, in which, the Jianshen 1 and Hanshen 1 Well Blocks were the sedimentation–subsidence centers and semi-deep lake subfacies were developed. Braided river delta deposits were widely developed in the Alaer area in the west and the Qiekelike area in the piedmont of the Kunlun Mountains. Fan deltas were distributed

in the Ganchaigou, Xianshuiquan and Yueyashan areas. Diluvial fans were chiefly developed in the Niubiziliang area of the piedmont of the Altun Mountains, Lulehe, Qianshan, Dongtai 1 Well Block, Mahai area and Yuanqiu 1 Well Block along the northern edge, and the Wutumeiren area along the southern margin of the Qaidam Basin. These diluvial fan fronts transitioned towards the center of the basin into contiguous braided river deposits. The eastern area underwent onlapping wedging-out during the period, and did not accept deposition. Flood plain deposits were widely developed in other areas within the basin (Fig. 11A).

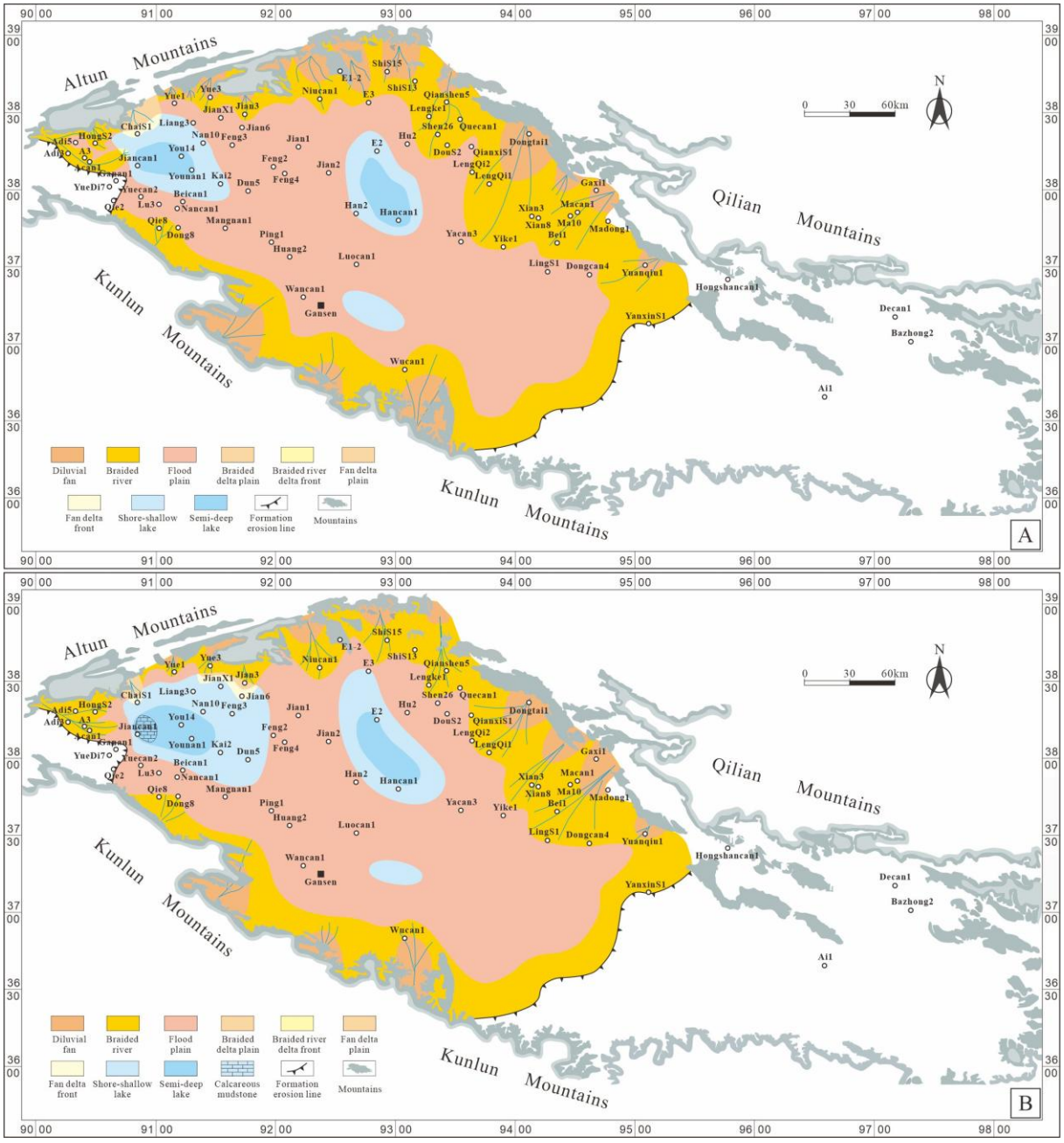


Fig.10 Lithofacies paleogeography map of Paleogene SQ1-SQ2 of the Qaidam Basin. (A) Lithofacies paleogeography map of Paleogene E_{1+2}-SQ1. (B) Lithofacies paleogeography map of Paleogene E_{1+2}-SQ2.

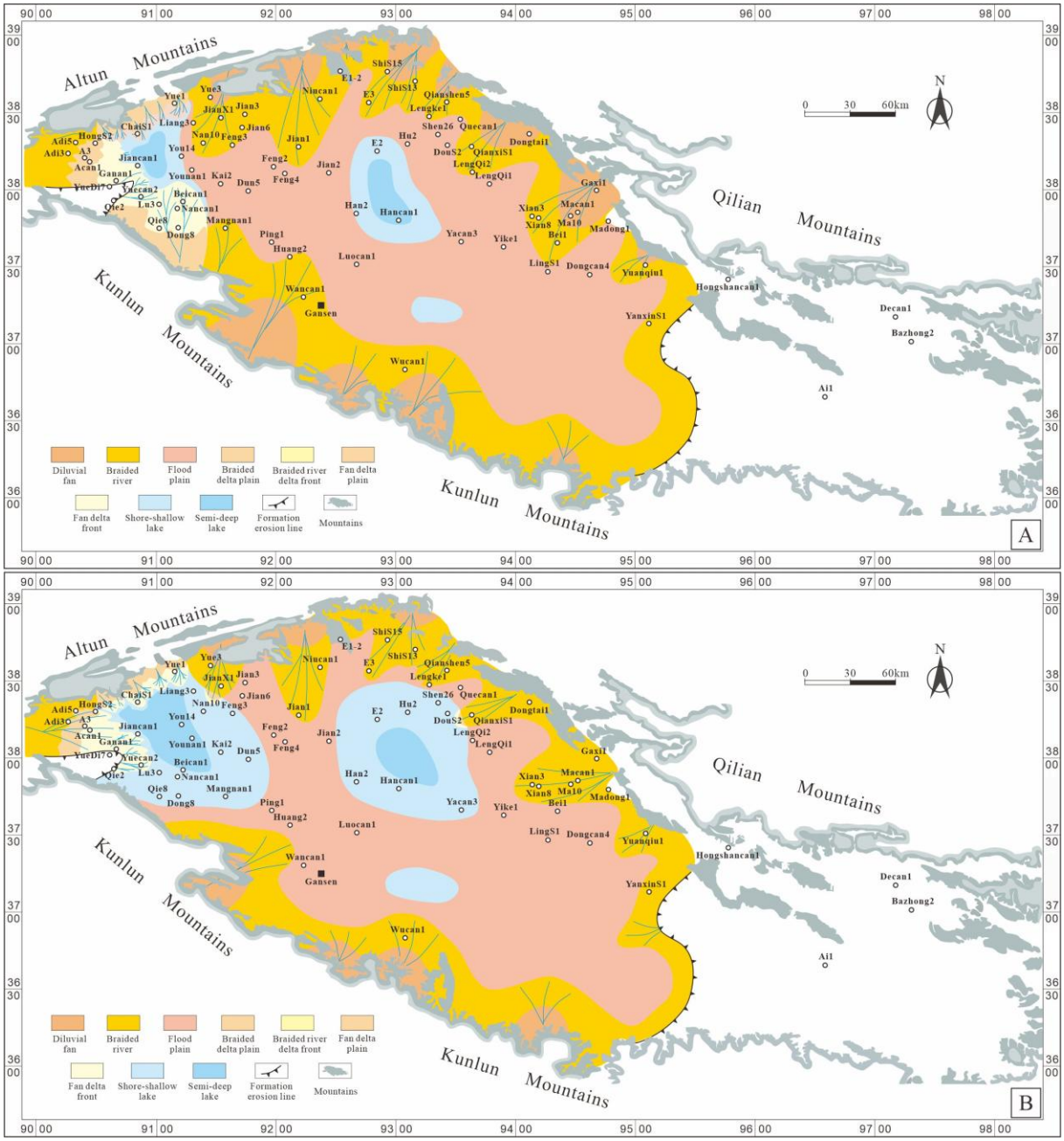


Fig.11 Lithofacies paleogeography map of Paleogene SQ3-SQ4 of the Qaidam Basin. (A) Lithofacies paleogeography map of Paleogene E_3^1-SQ3. (B) Lithofacies paleogeography map of Paleogene E_3^1-SQ4.

During the period of SQ4, the lake area was distinctly increased compared to that during the period of SQ3; the Youshashan and Yiliping areas were still the sedimentation–subsidence centers of the period, and semi-deep lake subfacies were developed. The semi-deep lake area

in the Youshashan area expanded to the Xianshuiquan and Shizigou areas. The shore–shallow lake expanded westwards to the edge of the Altun Mountains, southwards to the Alaer and Qiekelike areas, northwards to Dafengshan and eastwards to the Dun 5 and MN 1 Well Blocks. The shore–shallow lake area in the Yiliping area increased as well compared to that during the period of SQ3. Inherited fan delta deposits were developed in the Ganchaigou, Xianshuiquan and Yueyashan areas in the piedmont of the Altun Mountains in the western area, and diluvial fan deposits were developed in the Niubiziliang area. Braided rivers in the Alaer area flowed into the lake, forming braided river delta deposits. The piedmont of the Qilian Mountains along the northern edge was dominated by braided river deposits. Compared to SQ3, diluvial fan deposits were lacking and braided rivers near the Lenghu area flowed into the lake, forming braided river delta deposits. diluvial fans were developed in the Wutumeiren area along the southern margin and alluvial fan fronts were contiguous braided river deposits. Sedimentary facies distribution in other areas were basically consistent with that of the period of SQ3 (Fig. 11B).

4.4.3 SQ5-SQ6

During the depositional period of the Upper Member of the Lower Ganchaigou Formation (SQ5), the Qaidam Basin experienced large-scale lake transgression; the lake area expanded greatly, particularly the shore–shallow lake area. The two original shore–shallow lakes connected into a large-area shore–shallow lake. The shore–shallow lake had widened to the margin of the Altun Mountains westwards, northwards to the Dafengshan and Eboliang areas, southwards to the margin of the Kunlun Mountains and the Wanshen 1 Well Block, and eastwards to the Lenghu–Nanbaxian area. The semi-deep lake was still distributed in the

Youshashan and Yiliping areas, but the area was much larger than in SQ4. In addition, limy mudstone was developed in the Jianshen 1 Well Block in the semi-deep lake of the Youshashan area. The Hancan 1 and Han 2 Well Blocks in the Yiliping area had turned into semi-deep lacustrine deposits at that time. Due to the large slope in the Yueyashan area, diluvial fans entered into the lake and then quickly entered into the semi-deep lake, forming turbidity fan deposits. Fan deltas were contiguously developed in the western segment of the Altun Mountains. Braided river deltas were chiefly developed in the Jiandingshan, Dafengshan and Eboliang areas in the central segment of the Altun Mountains. The Qilain Mountains along the northern edge still lacked diluvial fan deposits and were dominated by braided river-braided river delta deposits. Diluvial fan–braided river deposits were developed in and to the west of the Wutumeiren area and along the southern edge. The eastern area started to accept deposits at that time. Except for braided rivers developed in piedmont zones, most areas were dominated by flood plain sediments. In addition, flood plain deposits were widely developed in other areas of the basin (Fig. 12A).

The southern boundary of the lake during the period of SQ6 retreated from the Gansen area to the Dafengshan area. The original Luocan 1 Well Block changed from a shore-shallow lake to a flood plain. The lake in the Leng 2 Well Block also retreated towards the center of the basin, turning the braided river delta present during SQ5 into a flood plain. The lake shore line in the Niubiziliang area directly advanced to the piedmont of the Altun Mountains, changing the diluvial fan-braided river-braided river delta present during SQ5 into a braided river front. Turbidity fan deposits developed in the semi-deep lake near Xianshuiquan and Yueyashan. Compared to SQ5, the Alaer area in the west changed from the original fan delta

into a braided river delta, and the Lenghu and Nanbaxian areas changed from the original braided river delta into a braided river-flood plain during this period. In the Huangshi and Wutumeiren areas along the southern edge, diluvial fan–braided river–flood plain deposits were developed. Sedimentary facies distribution in other areas are basically consistent with those of the period of SQ5 (Fig. 12B).

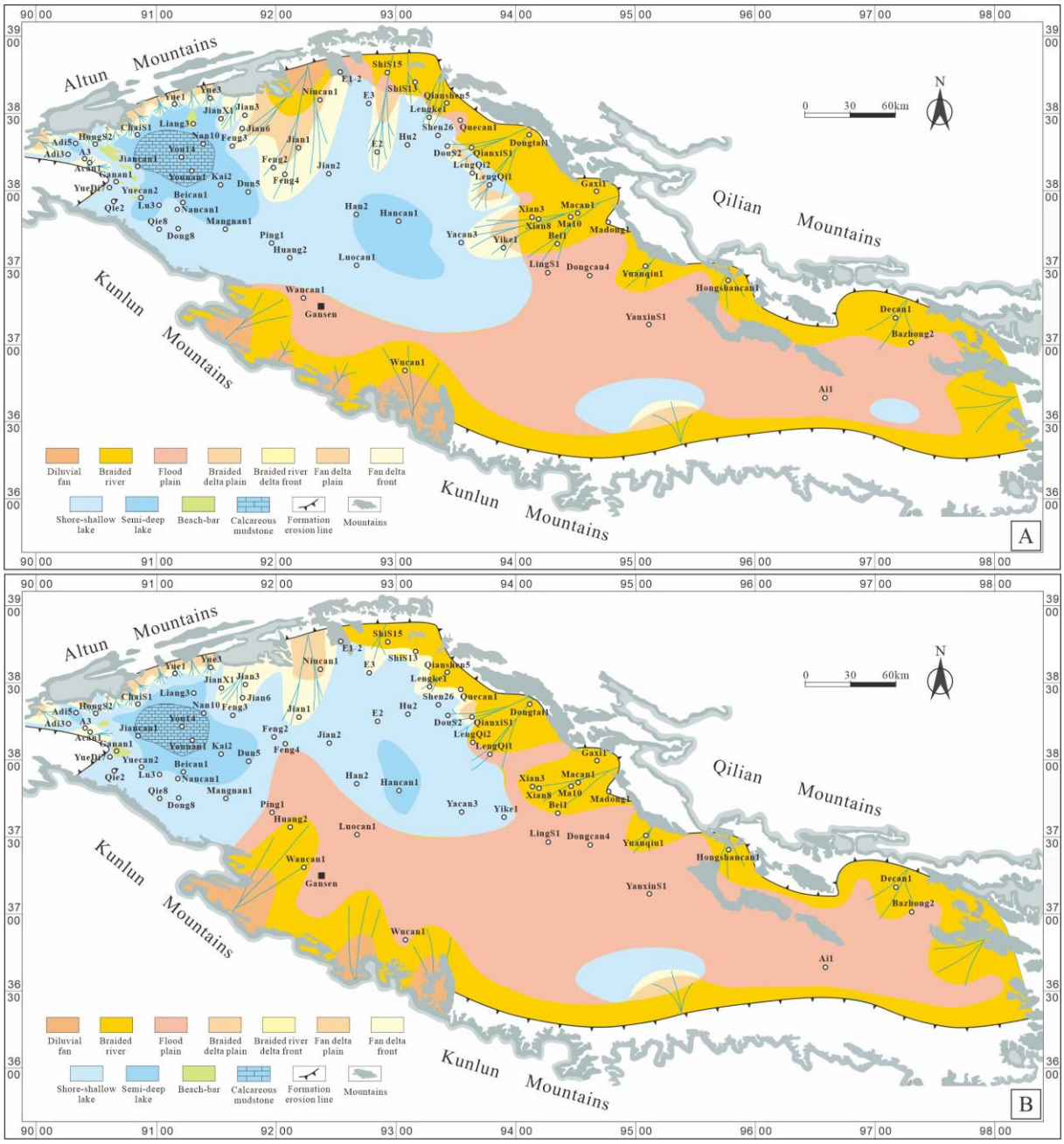


Fig.12 Lithofacies paleogeography map of Paleogene SQ5-SQ6 of the Qaidam Basin. (A)

Lithofacies paleogeography map of Paleogene E_3^2-SQ5. (B) Lithofacies paleogeography map of Paleogene E_3^2-SQ6.

4.4.4 SQ7-SQ8

During the depositional period of the Upper Ganchaigou Formation (SQ7), the Youshashan area, the Kai 2 Well Blocks and the Yiliping area were the subsidence centers, and semi-deep lake subfacies were developed. The Kai 2 and Dun 5 Well Blocks possessed limy mudstones. Large-area shore–shallow lake deposits were developed in the periphery of semi-deep lakes. In the Acan 1 Well Block of the west, diluvial fan deposits were developed, successively turning into diluvial fan–braided river–braided river delta–lake deposits towards the center of the basin. On steep slopes like Ganchaigou–Xianshuiquan–Yueyashan in the piedmont of the Altun Mountains, fan delta deposits were developed. In the Qiekelike area and the Mangnan 1 Well Blocks in the southwest, braided river delta deposits were developed. Diluvial fans were developed in the Dongtai 1 and Gaxi 1 Well Blocks along the northern edge. Braided river-braided river deltas were chiefly developed in the Lulehe and Lenghu areas. Braided river-flood plains were chiefly developed in the Maxian area. The southern edge was dominated by braided river-flood plain deposits. Diluvial fan deposits were developed in the Hcan 1 and Dcan 1 Well Blocks in the east, and contiguous braided river deposits were developed in the fronts. Flood plain deposits were widely developed in other areas of the basin (Fig. 13A).

During the period of SQ8, the lake area further expanded, and the eastern boundary of the shore–shallow lake expanded to the Luocan 1 and Yacan 3 Well Blocks. The northern boundary advanced towards the center of the basin, changing the Hu 2 Well Block from the

shore–shallow lake present during SQ7 into a flood plain. The Leng 2 Well Block in the northern edge changed from the braided river delta deposits present during SQ7 into a braided river. In the Alaer area of the west, braided river-braided river delta deposits were dominated. In the Xianshuiquan and Yueyashan areas, inherited fan delta deposits were developed. In the Huangshi area of the southwest, braided river-braided river delta deposits were developed. In the Dongtai 1 Well Block along the northern edge, inherited diluvial fans were developed. In the Huangshi area in the southwest, braided river-braided river delta deposits were developed. Inherited diluvial fans were developed in the Dongtai 1 Well Block along the northern edge, and diluvial fans transitioned towards the center of the basin into a widespread braided river, and then into a flood plain. Inherited braided river-flood plain deposits were developed along the southern edge, and diluvial fan-braided river-flood plains were developed in the east (Fig. 13B).

4.4.5 SQ9-SQ10

During the depositional period of the Lower Youshashan Formation (SQ9), the Youshashan and Yiliping areas were still the subsidence centers of the basin. The shore–shallow lake expanded northwards to the Hu 2 Well Block. The semi-deep lake area tended to increase and migrate eastwards relative to that in the SQ8 period. The semi-deep lake area in Youshashan expanded to the Dun 5 and Hanshen 1 Well Blocks, and that in Yiliping expanded as well. Limy mudstone was developed in Youshashan and the Mangnan 1 and Hanshen 1 Well Blocks. Inherited braided river-braided river deltas were developed in the Alaer area of the west. Inherited fan delta deposits were still developed in the Ganchaigou, Xianshuiquan and Yueyashan areas. Diluvial fan-braided river-braided river deltas were developed in the

Niubiziliang area. Braided river-braided river deltas were developed in the Huangshi area of the southwest. Inherited braided river-braided river deltas developed along the northern margin. During this period, the range of braided river deltas increased more than during SQ8. Braided river-flood plains were chiefly developed in the southern margin, diluvial fans developed in the Delingha area of the east, and inherited braided river deposits were developed in fronts of diluvial fans. Flood plains widely developed in other areas of the basin (Fig. 14A). During the period of SQ10, braided river deltas in the Huangshi area of the southwest totally transformed into shore–shallow lacustrine subfacies. The spreading of sedimentary facies in other areas is basically consistent with that of the period of SQ9 (Fig. 14B).

4.4.6 SQ11-SQ12

During the depositional period of the Upper Youshashan Formation (SQ11), the Upper Youshashan Formation suffered from intense denudation as intensely uplifted by three mountains in the periphery. Compared to the SQ10 period, the semi-deep lake area expanded, the original two semi-deep lakes connected into one large-area semi-deep lake, and limy limestone was developed in the semi-deep lakes of the Youshashan and Yiliping areas during the period of SQ11. The western and southern boundaries of the shore-shallow lake advanced towards the center of the basin, decreasing the sedimentary scope of fan deltas and braided river deltas in the piedmont of the Altun Mountains. Compared to the SQ10 period, during this period, braided river deltas disappeared in the Alaer area in the west, where braided rivers and flood plains were mainly developed. Fan delta sediments in the piedmont of the Altun Mountains decreased greatly and slightly developed in the Ganchaigou and Xianshuiquan

areas. Braided rivers and flood plains were chiefly developed in the Yueyashan area. Braided river deltas in the Jianshan and Dafengshan areas disappeared and semi-deep lake subfacies were developed. Braided river deltas in the Lenghu and Nanbaxian areas in the northern edge disappeared and large-scale flood plains were dominant. According to seismic facies and stratigraphic thickness, it is inferred that shore-shallow lake deposits were developed in the Yanxinshen 1 Well Block in the west and in the vicinity of the Ai 1 Well Block to the west. Xitieshan near the Yanxinshen 1 Well Block can be considered as braided river-braided river delta formed there by the provenance. Flood plain deposits were widely developed in other areas of the basin (Fig. 15A).

During the depositional period of the Shizigou Formation (SQ12), the lake area further expanded, and the northern boundary of the shore–shallow lake expanded to the Niushen 1-Hu 2-Lengqi 2-Xian 3-Bei 1-Dongshen 4 Well Blocks. The semi-deep lake area further expanded, and its northern boundary expanded to the Er 2 Well Block. Limy mudstone was developed in the Kai 2-Dun 5-Han 2 Well Blocks in the semi-deep lake. Braided river–braided river delta deposits were developed in the Alaer, Yueyashan and Shizigou areas in the west. During this period, the lake area was large, and the whole basin lacked diluvial fan and fan delta sediments, and surrounding the lake were wide flood plains and braided river deposits (Fig. 15B).

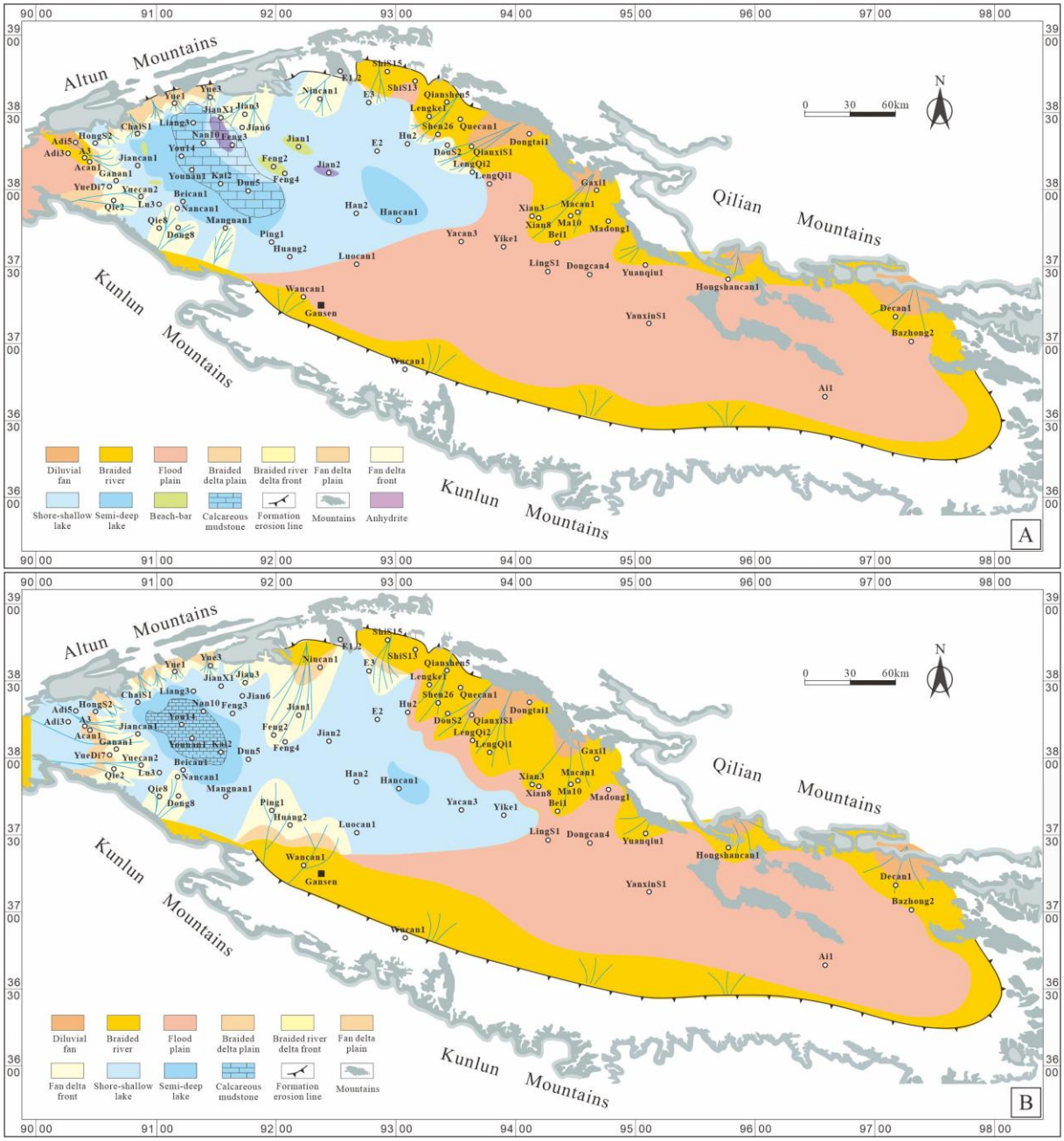
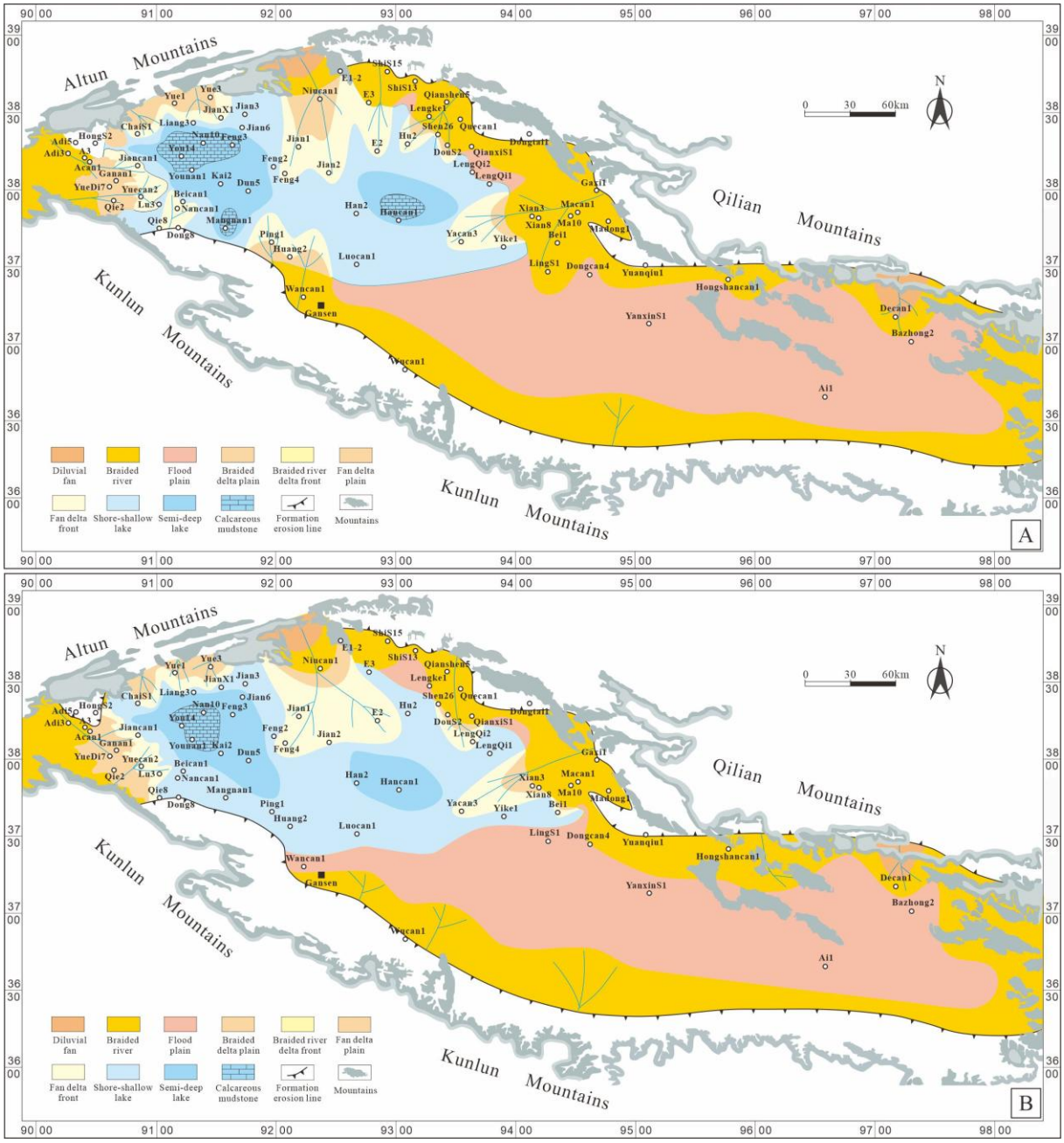


Fig.13 Lithofacies paleogeography map of Paleogene SQ7-SQ8 of the Qaidam Basin. (A) Lithofacies paleogeography map of Paleogene N_1-SQ7. (B) Lithofacies paleogeography map of Paleogene N_1-SQ8.



628

629 Fig.14 Lithofacies paleogeography map of Paleogene SQ9-SQ10 of the Qaidam Basin. (A)

630 Lithofacies paleogeography map of Paleogene N_2^1-SQ9. (B) Lithofacies paleogeography map

631 of Paleogene N_2^1-SQ10.

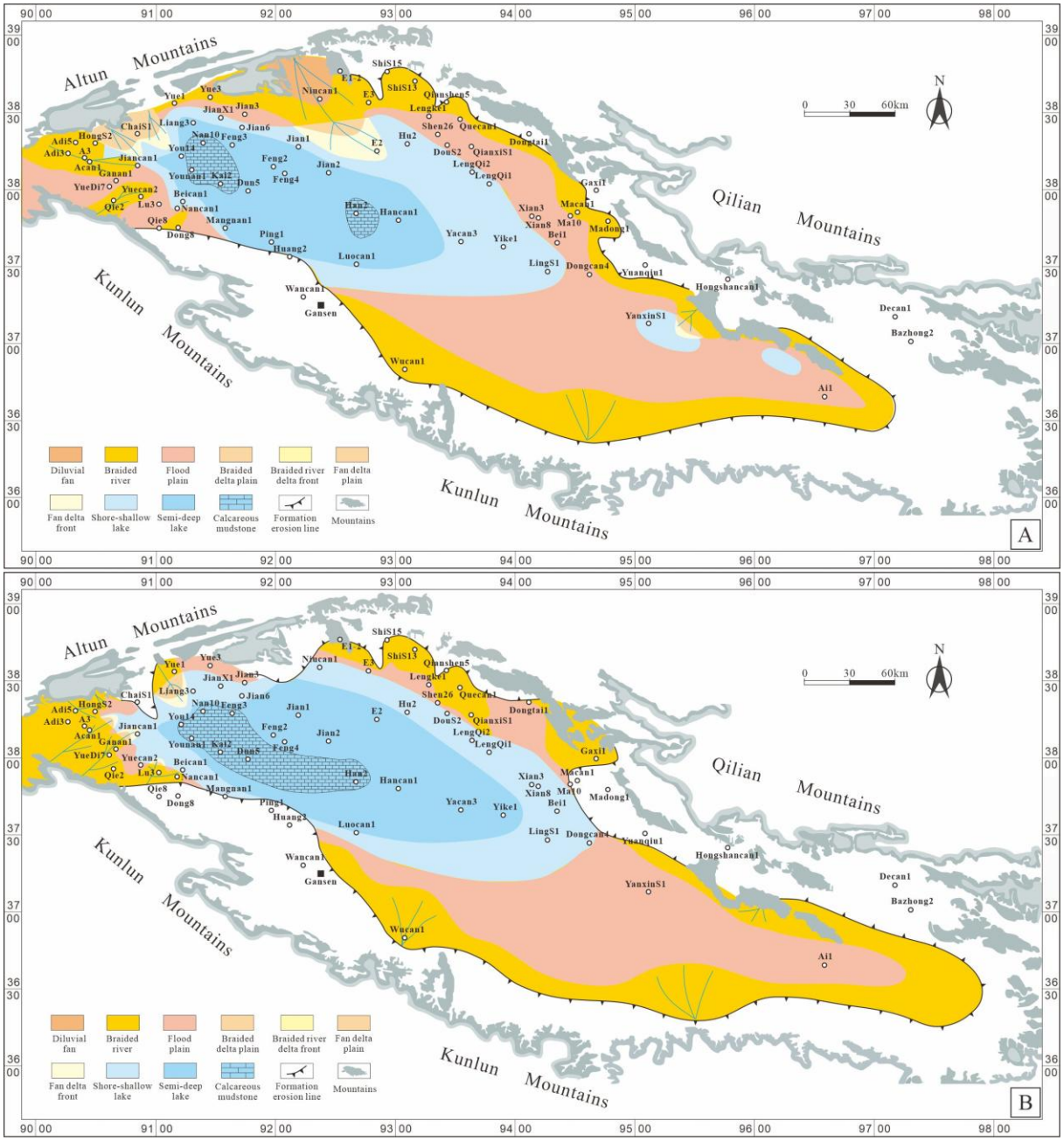


Fig.15 Lithofacies paleogeography map of Paleogene SQ11-SQ12 of the Qaidam Basin. (A) Lithofacies paleogeography map of Paleogene N_2^2-SQ11. (B) Lithofacies paleogeography map of Paleogene N_2^3-SQ12.

4.5 Source rocks and reservoirs

4.5.1 Source rocks

Lacustrine mudstones are the main hydrocarbon source rocks in continental basins (Zhu

et al., 2004; Shan et al., 2013; Zhao et al., 2015; Ding et al., 2016). In Tertiary argillaceous source rocks of the Qaidam Basin, the total organic carbon content (TOC) varies from 0.15% to 4.5%, with an average of ~0.3%, mostly <0.5%. Lake argillaceous source rocks in eastern China mostly have a TOC of >1.5% (Table 5). Tertiary lake waters of the Qaidam Basin are generally shallow, lacking deep-lake deposits; mudstone is usually interbedded with siltstone and fine sandstone and shale are not developed. In addition, due to intense evaporation during the evolution process of Cenozoic lakes, the lake level fluctuated intensely and frequently and semi-deep lakes often changed into shallow lakes and even became dry. Thus, shallow and semi-deep lakes usually alternate frequently in cross sections, leading to a vertical difference in the TOC of mudstone.

Table 5

Lacustrine source rock organic carbon and other oil generation index from some basin of China. According to the Petroleum Geology of China (Annals).

Basin	Formation	Lake type	TOC /%	Chloroform asphalt "A" /%	Total hydrocarbon （ppm）
Songliao Basin	Cretaceous	freshwater lake	2.21		1612
Liaohe Depression	Paleogene	freshwater lake	2.55	0.2370	
Qikou Sag of Huanghua Depression	Paleogene	freshwater lake	1.48	0.1840	
	Paleogene	freshwater lake	1.62	0.2290	
Dongying Sag of Jiyang Depression	Paleogene	freshwater lake	1.66	0.2400	1060
Biyang Basin	Paleogene	salt water lake	1.83	0.2168	1219
Qaidam Basin	Paleogene	salt water lake	0.40		
	Neogene	salt water lake	0.30		

653 The Tertiary lake of the Qaidam Basin is a typical salt water lake. According to the
654 Petroleum Geology of China (Annals), comparison with the TOC of argillaceous sediments of
655 some modern freshwater lakes and salt water lakes and oceans (their salinities are equivalent
656 to those of salt lakes) across the globe indicates that the salinity of lake water poses weak
657 influences on organic abundance (Table 6). However, salinity affects organic types. The
658 higher the salinity, the better the organic type, and the higher the oil generation capability
659 (Ramona et al., 2017). Organic matter from lake aquatic life is mostly I-type, and that brought
660 by rivers is mostly III-type. Due to the Qaidam Basin possessing a dry climate during the
661 Tertiary Period, vegetation was not developed, organic matter from rivers was small in
662 number, organic matter of lacustrine mudstone was mainly from the inside of lakes, and the
663 organic matter types were favorable. This may result in the organic abundance of lacustrine
664 sources of the Qaidam Basin being low, but the source rocks have comparatively high oil
665 generation capability.

666 Table 6

667 TOC content in typical saline lake, freshwater lake and marine muddy sediments. According
668 to the Petroleum Geology of China (Annals).

Lake	Qinghai Lake	Caspian Sea	Balkhash Lake	Erie lake	Hughes lake	Baikal lake	Black Sea	Shallow Pacific
TOC /%	2.30	2.10	1.00	2.50	2.70	2.10	1.80	0.40
Salinity /%	1.24	1.25	0.15～0.50	0.01	0.01	0.01	1.75	3.50
Type	salt water lake	salt water lake	brackish water lake	freshwater lake	freshwater lake	freshwater lake	salt water lake	seawater

669 According to the sedimentary system distribution of various sequences in combination
670 with the TOC measurement of mudstone samples, the distribution of source rocks was

identified. The lake area expanded from the Lulehe Formation to the Shizigou Formation, reflecting the gradually increasing distribution scope of source rocks. In the depositional period of the Lulehe Formation and the Lower Member of the Lower Ganchaigou Formation, two separate, small-area lakes were developed, of which, one was located in the Mangya Sag of the southwestern basin and the other was located in the Yiliping Depression. From the Upper Member of the Lower Ganchaigou Formation to the Shizigou Formation, the two lakes connected as one, and the area gradually increased. From SQ5 to SQ11, although the lakes were contiguously distributed, the semi-deep lakes did not connect as one, and there were consistently two sedimentary centers. According to burial depth and vitrinite reflectance, source rocks from the Upper Member of the Lower Ganchaigou Formation (SQ5 and SQ6) to the lower part of the Upper Ganchaigou Formation (sequence SQ7) in the Mangya sag entered into the hydrocarbon generation window. They are thick and widespread and are the dominant source rocks. The Yiliping depression has more petroleum source beds and thicker source rocks than the Mangya sag. Source rocks of the Lower Member of the Lower Ganchaigou Formation to the Lower Youshashan Formation all entered into the hydrocarbon generation window and became the dominant source rocks of the depression.

4.5.2 Reservoirs

The economically important reservoirs in the Tertiary strata of the Qaidam Basin are composed of coarse deposits such as conglomerates and sandstones. In addition, some areas have minor carbonate reservoirs. Clastic rock reservoirs are formed mainly in diluvial fan, fan delta, braided river, braided river delta and shore-shallow lake environments. Clastic rock reservoirs are developed in various horizons, and in plan view are chiefly distributed along

693 the margin of the basin. Clastic rock reservoirs in various horizons have different distribution
694 ranges. In the Lulehe Formation (SQ1 and SQ2) and the Lower Member of the Lower
695 Ganchaigou Formation (SQ3 and SQ4), diluvial fan and braided river facies reservoirs are
696 mainly developed along the margin of the basin with a 20-50 km width. Fan delta reservoirs
697 are mainly developed in the piedmont of the Altun Mountains and braided river delta
698 reservoirs are developed in the Alaer and Qiekelike areas. From the Upper Member of the
699 Lower Ganchaigou Formation (SQ5 and SQ6) to the Lower Youshashan Formation (SQ9 and
700 SQ10), braided river delta reservoirs were widely developed as the lake expanded,
701 surrounding the lake to the north, west and south. To the east of the lake, due to no river
702 injection, deltas were not developed. Diluvial fan and braided river reservoirs were still
703 developed along the basin margin. During this period, the clastic rock facies zone was wide as
704 well at approximately 20-50 km. From the Upper Youshashan Formation (SQ11) to the
705 Shizigou Formation (SQ12), the clastic rock facies zone in the basin became narrow, with a
706 width of approximately 20 km, and was dominated by braided river reservoirs.

707 Reservoir microscopic experiments and reservoir physical property analysis indicate that
708 the reservoirs in the Qaidam Basin have vastly different quality controls from freshwater lake
709 reservoirs. In freshwater lakes, delta front and shore-shallow beach bar sands generally have
710 better structure, lower matrix content and better physical properties than fluvial sandstone and
711 delta plain sandstones due to long-term washing by lake waves. But in salt water lakes,
712 calcium carbonate and sulfate precipitated positively, leading to intense reservoir cementing
713 due to intense evaporation. Therefore, delta front and shore-shallow lake beach bar sand
714 reservoirs have worse physical properties than fluvial facies sandstone and delta plain

715 sandstone reservoirs. In plan view, reservoirs in the northern margin have optimum quality,
716 followed by those in the Alaer area in the southwestern Qaidam Basin. These reservoirs are
717 mainly braided river or braided river delta plain sediments, and other areas are mostly braided
718 river delta front or fan delta front sediments, with poor reservoir physical properties. In the
719 Lenghu to Nanbaxian areas, E_3^1~E_3^2 reservoirs have porosities mostly varying from 15%-25%
720 and permeability of up to several hundreds to thousands of millidarcies. The reservoirs in the
721 Alkun slope in the southwestern Qaidam Basin have porosities mostly of 10%-18% and
722 permeabilities mostly of <10 millidarcies. Lake and delta front sediments have electrical
723 resistivities higher than braided river and braided river delta plains, as is the case with the
724 Hong33 and Hong18 Wells.

725 **5. Discussion**

726 *5.1 Controlling factors of lithofacies paleogeography*

727 On the basis of sequence stratigraphy and the study of sedimentary facies evolution,
728 from the perspective of paleo-climate and basin evolution, the controlling factors on
729 sedimentary systems were summarized and the coupling relationship between lake basin
730 evolution and lithofacies paleogeography was discussed.

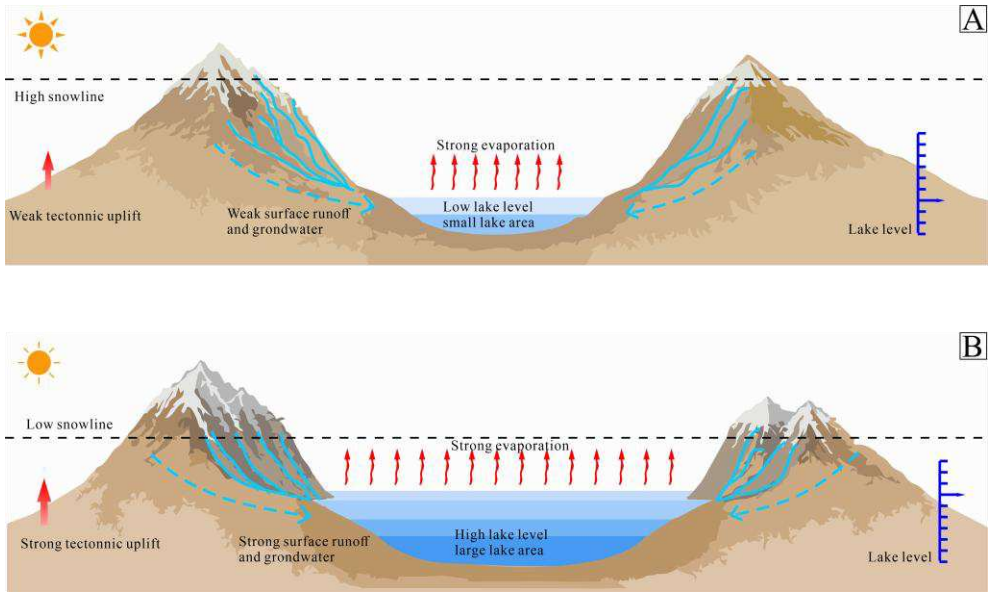
731 *5.1.1 Relationship between paleo-climate and lithofacies paleogeography*

732 In various periods of the Paleogene–Neogene, the lake scale was variable in the Qaidam
733 Basin. Previous scholars proposed that lake area is controlled by changes in climate: in a dry
734 climate the lake area is small, and in a wet climate the lake area is large. According to this
735 view, maximum lake transgression should occur during the period with the wettest climate,
736 maximum rainfall and minimum salinity. However, evaporaites were most developed in the

maximum Tertiary lake transgression period of the basin. Lithologic, paleontological and geochemical evidence shows that the Tertiary climate of the Qaidam Basin was consistently dry, with evaporation capacity much higher than rainfall. This being the case, we must ask: In a dry climate background, where does lake water come from, and what are the controlling factors of lake scale?

The answer to these questions can be found in mountain snow. Lake water in dry climate areas of western China mainly comes from the snowmelt of mountainous areas, which can be seen in modern Qinghai Lake and Persia Lake in Xinjiang (Farinotti et al., 2015; Li et al., 2021; Immerzeel et al., 2020). Qinghai Lake is mainly supplied by river water, followed by lake-bottom springs and rainfall. The rivers and lake-bottom springs are fed by melted snow from the mountainous areas. Persia Lake in Xinjiang receives the majority of its water from the Kaidu and Malasitai rivers in the northwest, and this river water is chiefly supplied by snowmelt from the Tianshan Mountains. In addition to the Qinghai and Persia lakes, lakes currently located in the Qaidam Basin, such as the Dabuxun and Gasikule lakes, are also mainly fed by snowmelt from the mountains. The number of Tertiary lakes in the Qaidam Basin is correlated to the snowmelt of mountainous areas, while the amount of snowmelt is correlated to the height and temperature of the mountains surrounding the basin. More water is produced if the mountain height is high, the climate is cold and the area above the snowline is large (Fig. 16). Mountain height is correlated to tectonism intensity. When tectonism intensity and the amplitude of mountain uplifting are greater, a larger area will be located above the snowline. Moreover, there will be more accumulated snow and a greater volume of snowmelt. If mountains surrounding lakes in a dry climate area are far below the snowline,

759 there will be no accumulated snow present year round. In winter, the snow will quickly
760 evaporate, resulting in a lack of snowmelt to supply nearby lakes with water.



761

762 Fig.16 Tertiary snowmelt-fed lake model in the Qaidam Basin: correlation between
763 snow-capped mountain elevation and lake level fluctuations.

764 *5.1.2 Relationship between mountain height and lake area*

765 From the perspective of sedimentary facies distribution of various sequences in the
766 Qaidam Basin, the Tertiary lake was in a maximum lake transgression period during the
767 depositional period of the Upper Youshashan Formation–Shizigou Formation, during which
768 time the lake area reached its maximum size. The Tertiary Period generally was a large lake
769 transgression cycle. Due to the continuous action of regional tectonic stress, the mountains
770 surrounding the Qaidam Basin gradually rose, the snow covered areas continuously expanded,
771 and the volume of snow continued to increase. In the depositional period of the Lulehe
772 Formation to the Lower Member of the Lower Ganchaigou Formation, the lake area was
773 small. This is mainly because this was the initial period during which the mountains
774 surrounding the basin were not high and the area above the snowline was small. In addition,

775 sporopollen research indicates that the climate during this period was dry and hot and that the
776 snowline elevation above sea level was much higher (Sun et al., 2010; Fang et al., 2020).
777 These factors were not favorable for the accumulation of snow. Therefore, only a limited
778 amount of snowmelt was supplied into the basin via surface rivers or artesian ground springs,
779 giving rise to very small lakes. During the depositional period of the upper part of the Lower
780 Member of the Lower Ganchaigou Formation to the Shizigou Formation, the lake area began
781 to enlarge. The cause of this is twofold. Firstly, the mountains surrounding the basin rose
782 continuously. Secondly, the climate shifted from dry and hot to dry and cold, decreasing the
783 elevation of the snowline. These two factors led to an expanded area in which snow could
784 accumulate, as well as an increase in snowmelt; thus the lake area continuously expanded (Fig.
785 16).

786 The Cenozoic differential uplift of peripheral mountain ranges (e.g., Altun Shan and
787 Qilian Shan) created significant topographic relief (>2000 m) along the basin margin, where
788 intense frost weathering generated abundant angular detritus. Seismic profiles reveal
789 wedge-shaped progradational clinoforms (4-7° dip angles) along the basin periphery,
790 corresponding to staged progradation of glaciofluvial fan systems. In the Upper Member of
791 the Lower Ganchaigou Formation, conglomeratic units contain quartz grains exhibiting
792 characteristic glacial striations (as evidenced by SEM microtextures) (Smith et al., 2020),
793 while detrital zircon U-Pb age spectra demonstrate that 50-60% of sediment provenance
794 derived from newly uplifted Mesozoic granitic bedrocks, indicating that tectonic uplift
795 directly controlled bedrock exposure in source areas. This synergistic mechanism shows that
796 tectonic uplift governed sediment supply potential through topographic construction, while

797 climatic fluctuations regulated meltwater transport efficiency via snowline altitude variations.
798 Their combined effects drove the transformation of depositional systems from early-stage
799 confined fluvial-alluvial systems (sandstone/conglomerate >70%) to late-stage extensive
800 lacustrine environments (mudstone >60%). This evolutionary pattern serves as a
801 quintessential example of the tripartite coupling process involving "tectonic uplift-climatic
802 variation-basin infilling" along the northern margin of the Tibetan Plateau.

803 *5.1.3 Correlation between basin evolution and sedimentary systems*

804 The Qaidam Basin was reworked by multi-phased tectonic movement, which had a
805 major influence on the sedimentation evolution process. During the late Eocene, there were
806 two subsidence centers, i.e., the Mangya sag and the Yiliping depression. The Mangya sag
807 occurs as a NW-elongated band, with a maximum sedimentary thickness of approximately
808 2000 m. The Yiliping depression is under a general depression background and shows local
809 faulting characteristics, with a maximum thickness of 2700 m. In addition to the above two
810 subsidence centers, as controlled by piedmont faults, there were two small-area subsidence
811 centers in the Nuomuhong and Germu areas in the piedmont of the Kunlun Mountains. Due to
812 variations in tectonism type and intensity, the subsidence centers migrated. During the
813 depositional period of the Upper Ganchaigou Formation, the whole western Qaidam area was
814 uplifted and the subsidence centers migrated greatly eastwards. During the late Miocene, the
815 Yiliping subsidence centers greatly shifted southeastwards. The Shizigou Formation was
816 intensely denuded in the west and northern margin, and the subsidence centers migrated to the
817 Yikeyawuru and Tainan areas, thus forming the Sanhu depression.

818 With the uplifting force from the Tibetan Plateau, the Qaidam Basin continued to be

819 squeezed in a NW direction during the Tertiary Period, and the basin marginal faults formed
820 during different periods shifted into different positions, leading to different basin scales and
821 variable basin boundaries. During the depositional period of the Lulehe Formation to the
822 Upper Member of the Lower Ganchaigou Formation, the southern and northern boundaries of
823 the basin retreated continuously, and the basin scale expanded continuously, forming an
824 upward deepening and fining sedimentary sequence. Basin boundary retreating was mainly
825 aroused by boundary fault retreating in a step-like way (Fig. 17). During the depositional
826 period of the Upper Ganchaigou Formation to the Lower Youshashan Formation, the southern
827 boundary of the basin advanced continuously towards N and the center of the basin, which led
828 to a gradual coarsening of the lithography in the stratigraphic section of the west. This
829 boundary advancing was mainly aroused by the step-like advancing of boundary faults (Fig.
830 17). This step-wise fault displacement critically controlled depositional systems by
831 modulating accommodation space creation and provenance supply pathways, as evidenced by
832 the migration of alluvial fan aprons along reactivated fault scarps and compartmentalized
833 distribution of lacustrine facies between fault-controlled sub-basins. The Cenozoic tectonic
834 evolution of the Qaidam Basin features two distinct phases: (1) An early extensional phase
835 (50–35 Ma) dominated by SW-directed listric normal faulting along the Altyn Tagh strike-slip
836 system (slip rates 0.3–0.5 mm/yr), driving stepwise basin boundary retreat and depositing
837 800–1200 m of upward-fining deep lacustrine facies with high accommodation/sediment
838 supply (A/S) ratios (>2.5); (2) A late compressional phase (35–15 Ma) transitioning to a
839 NE-directed thrust-dominated regime (slip rates 0.2–0.3 mm/yr), which induced northward
840 basin boundary advance and accumulated 600–800 m of upward-coarsening braided delta

complexes under low A/S conditions (<1). Slip rate thresholds quantitatively constrain tectonic-sedimentary coupling, providing predictive insights for hydrocarbon source-reservoir configurations.

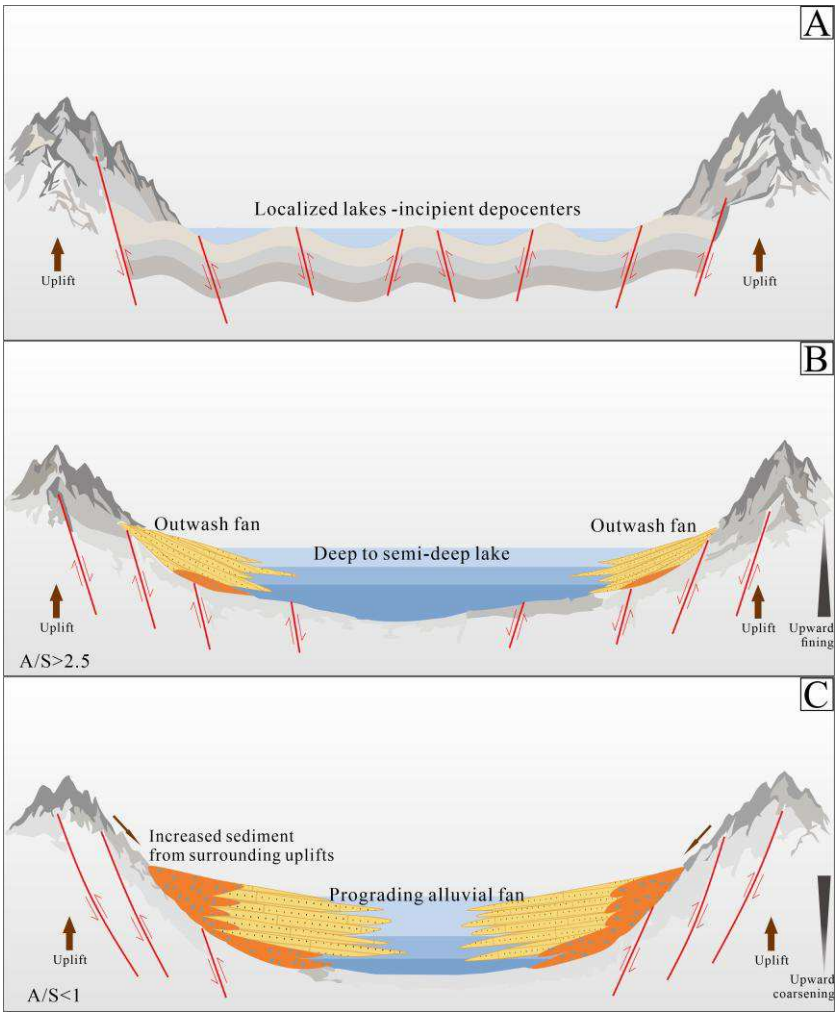


Fig.17 Control of Lake Basin Dimensions by Episodic Fault Activity in the Tertiary of Qaidam Basin. (A). The initial formation of the Qaidam Basin. (B). Boundary faults recede and the basin expands. (C). Boundary faults push into the basin and the basin shrinks.

Based on the distribution of sedimentary system in each sequence period and the tectonic evolution history of the basin, the relationship between tectonic evolution and sedimentary system of Tertiary is summarized. During the depositional period of the Lulehe Formation, the basin was compressed by the NW-trending movement of the Tibetan Plateau, forming two

852 subsidence centers in the Shizigou–Mangya sag in the south and the Yiliping depression in the
853 north. During this period, the peripheral mountain systems were not very high and the area for
854 snow accumulation was small; thus, less water flowed into the basin, resulting in the
855 formation of small-area lakes. During the initial period of the Lower Ganchaigou Formation,
856 under a continuous squeezing stress, the basin boundary advanced towards the center of the
857 basin, forming large-scale conglomerate in the basin margin. During the depositional period
858 of the Upper Member of the Lower Ganchaigou Formation, the basin retreated continuously,
859 expanding the basin scale and forming an upward fining sedimentary sequence of the Lower
860 Ganchaigou Formation. During this period, the peripheral mountain systems were uplifted
861 continuously and the snow covered also continuously expanded. As a result, more water
862 flowed into the basin and the lake area expanded continuously. During the depositional period
863 of the Upper Ganchaigou Formation, the southern boundary of the basin migrated greatly
864 northwards, leading to the Upper Ganchaigou Formation river and delta coarse-grained
865 sediments to be covered on E_3^2 semi-deep lacustrained dark-colored fine-grained sediments.
866 Then, the southern margin continued to migrate northwards in a step way. Towards the end of
867 the depositional period of the Lower Youshashan Formation, the basin margin was uplifted
868 greatly and suffered denudation, forming the regional unconformity between the Upper and
869 Lower Youshashan Formations. From the Upper Youshashan Formation to the Shizigou
870 Formations, the basin continued to subside, the peripheral mountains continued to be uplifted,
871 and the land of snow expanded. As such, the flow of water continuously increased and the
872 lake area also continuously expanded. The tectonic movement at the end of the Tertiary
873 Period caused the basin to suffer large-scale compression and uplifting once more, forming

874 the regional unconformity between the Neogene and the Quaternary periods.

875 *5.2 Hydrocarbon exploration potentials*

876 Source rock and reservoir qualities are the most important factors for hydrocarbon
877 evaluation in petroliferous basins. The configuration relationship between development facies
878 zones of source rocks and reservoirs was analyzed from the perspective of lithofacies
879 paleogeography in order to predict favorable hydrocarbon-bearing zones. Tertiary
880 hydrocarbon distribution in the Qaidam Basin shows typical patterns, i.e., the Tertiary
881 hydrocarbons mainly surround the hydrocarbon generation centers of semi-deep lakes (Wang
882 et al., 2015). For example, the oil and gas fields discovered in the southwest all surround the
883 Mangya depression. The major source rocks are E_3^2 semi-deep lacustrine, dark-colored
884 mudstones and argillaceous marl-limestones. N_1 and N_2 also have large-scale semi-deep lakes,
885 but source rocks in the most area are not mature; thus they cannot generate massive amounts
886 of oil and gas.

887 Research into sedimentary facies of various sequence periods indicates that the Tertiary
888 has two semi-deep lake development zones, i.e., the Mangya sag and the Yiliping depression
889 in the southwest. The Mangya sag peripheral, i.e., the Kunbei slope and the Altun slope, have
890 widespread deltas, where sands closely surround hydrocarbon generation centers and directly
891 insert into source rocks, enjoying the advantage of “being in a favored position”. Thus, the
892 Kunbei and Altun slopes are optimum exploration zones. The Kunbei slope has a series of
893 NW-SE trending faults, while banded delta sands strike NE-SW in this area. Therefore, the
894 sands in the periphery of the depression combine well with the faults in terms of striking, and
895 the sands are mostly transected and sealed by the faults, forming fault-lithology traps. In the

Altun slope, multiple fault-lithology traps occur below reverse faults, so this slope is a favorable exploration target of the area.

Semi-deep lakes have been developed for the long term in the Yiliping depression, and it is a significant hydrocarbon generation center in the basin. In this depression, not only have E_3^2 source rocks have entered into a mature stage, but N_1 and N_2 source rocks are also below a depth of 3000 m and have entered into a mature stage. However, large-scale fluvial facies sands of the Yiliping depression have mostly not entered into semi-deep lacustraine source rocks. The reservoirs and the source rocks are hindered by flood plain facies mudstones, and the generated oil and gas hardly enter directly into traps along sand beds. The main pathways for oil and gas migration are faults. Thus, vicinities of large faults that are transverse to hydrocarbon generation depressions are favorable exploration targets.

Recent hydrocarbon discoveries in the Qaidam Basin have further validated the spatial correlation between depositional systems and petroleum distribution. The Kunbei Slope has revealed the Kunbei oilfield cluster (e.g., Well Qietan-1 and Qietan-2) with proven reserves exceeding 100 million tons. High-productivity reservoirs predominantly occur in E_3^2 delta front sand bodies, where NW-SE trending faults truncate sandy deposits to form fault-lithologic traps. Source rock maturity (Ro=0.8%-1.2%) exhibits positive correlation with burial depth (>3500m). In the Altun Slope, the Dongping gas field demonstrates hydrocarbon migration through "fault-sandbody conduits", where thrust faults connect deep mature E_3^2 source rocks (Ro>1.0%) with shallow fan-delta reservoirs in N_1 sequences. Notably, the newly discovered Jianbei deep biogenic gas reservoir (4500m depth) in Yiliping Depression highlights accelerated maturation of N_2 semi-deep lacustrine source rocks due to rapid

subsidence (geothermal gradient 3.2℃/100m), achieving maturity threshold (Ro=0.7%) as early as the Early Pleistocene. However, limited lateral connectivity of fluvial sand bodies restricts gas accumulation strictly along major fault zones.

6. Conclusions

In this paper, a series of sequence stratigraphy, sedimentary systems and the hydrocarbon exploration potential of the Tertiary in the Qaidam Basin were studied through descriptions of outcrops and cores; analyses of log data; and interpretations of 3-D seismic profiles. A number of points are determined as follows:

(1) Based on regional and local unconformities, seven second-order sequences and twelve third-order sequences were identified in the Tertiary in the Qaidam Basin. Several system tracts in third-order sequences were also recognized on the basis of log patterns, seismic responses and sedimentary successions. By integrating multi-scale unconformity surfaces with system tracts identified through log-seismic-sedimentological analysis, this approach resolves universal challenges in correlating syn-rift stratigraphy, particularly in basins experiencing pulsed tectonic activation.

(2) Sedimentary systems of the Tertiary include diluvial fan, braided river, flood plain, fan delta, braided river delta, lake and turbidite fan. The distribution characteristics and evolution of each sedimentary facies in the third-order sequences were summarized, using the single-factor analysis and multi-factor comprehensive mapping method. All kinds of sedimentary facies are mainly distributed in the western part of the basin, while the eastern part is dominated by braided river and flood plain.

(3) In the Qaidam Basin, organic matter of the Tertiary lacustrine mudstone was mainly

from the inside of lakes, and the organic matter types were favorable. Source rocks from the Upper Member of the Lower Ganchaigou Formation to the lower part of the Upper Ganchaigou Formation in the Mangya sag, and Lower Member of the Lower Ganchaigou Formation to the Lower Youshashan Formation in the Yiliping depression are the dominant source rocks in the Qaidam Basin. The Tertiary reservoirs in the Qaidam Basin are composed of coarse deposits such as conglomerates and sandstones. In plan view, reservoirs in the northern margin have optimum quality, followed by those in the Alaer area in the southwestern Qaidam Basin.

(4) The Qaidam Basin was reworked by multi-phased tectonic movement, which had a major influence on the sedimentation evolution process. During the Tertiary period, the mountains surrounding the Qaidam Basin gradually rose, the snow covered areas continuously expanded; thus the lake area expanded continuously. Tertiary hydrocarbons mainly surround the hydrocarbon generation centers of semi-deep lakes. The Shizigou–Mangya Sag is the most optimal exploration zone, characterized by a proven "source-reservoir-seal integration", where deltaic sands and fault networks create effective hydrocarbon traps. With optimal spatial coupling between mature source rocks (Ro > 0.8%) and reservoirs, this area warrants prioritized development drilling. In contrast, the Yiliping depression center is a potential favorable exploration zone. Despite hosting mature source rocks, critical challenges persist, including heterogeneity in reservoir-caprock assemblages and incomplete fault migration systems. Realizing its resource potential requires advanced 3D seismic characterization to resolve the spatial interplay between sand bodies and faults.

Funding

This work was supported by the National Natural Science Foundation of China (41702158), the Natural Science Foundation of Shandong Province (ZR2022MD014), and the Fundamental Research Funds for the Central Universities (18CX02057A).

Acknowledgements

We are grateful to Prof. Youliang Ji and Prof. Dakang Zhong for their constructive advice on the framework of this study.

References

Jolivet, M., Brunel, M., Seward, D. (2001). Tectonics of the northern Tibetan Plateau: Insights from the Qaidam Basin and implications for hydrocarbon exploration. Tectonophysics. 343(1–2), 31-58.

Ritts, B. D., Hanson, A. D., Darby, B. J. (2008). Sedimentary and tectonic evolution of the Qaidam Basin, China: Implications for the petroleum system. AAPG Bulletin. 92(7), 887-911.

Zhang, Y., Wang, X., Liu, C. (2020). Tectonic evolution and hydrocarbon accumulation in the western Qaidam Basin, NW China. Marine and Petroleum Geology. 122, 104634.

Liu, H., Jin, Z., Li, P. (2021). Reservoir characteristics of tight sandstone gas in the northern Qaidam Basin. Journal of Petroleum Science and Engineering. 205, 108937.

Zavala, C., Arcuri, M. (2016). Intrabasinal and extrabasinal turbidites: Origin and distinctive characteristics. Sedimentary Geology. 337, 36-54.

Cai, Q.S., Hu, M.Y, Ngia, N.G., Hu, Z.G. (2017). Sequence stratigraphy, sedimentary

983 systems and implications for hydrocarbon exploration in the northern Xujiaweizi Fault
984 Depression, Songliao Basin, NE China. Journal of Petroleum Science and Engineering. 152,
985 471-494.
986 Song, F., Su, N.N, Kong, X.W., Liu, C.J., Song, C.F. (2020). Sedimentary characteristics
987 of humid alluvial fan and its control on hydrocarbon accumulation: A case study on the
988 northern margin of the Junggar Basin, west China. Journal of Petroleum Science and
989 Engineering. 187, 729-743.
990 Metivier, F., Gaudemer, Y., Tapponnier, P. (1998). Northeastward growth of the Tibet
991 Plateau deduced from balanced reconstruction of two depositional areas: The Qaidam and
992 Hexi Corridor basins, China. Tectonics. 17, 823-842.
993 Guo, S.B., Chen, C.L. (2008). Sequence stratigraphy of Quaternary Seven Spring Group
994 of the Sanhu Depression and prediction for prospective targets for hydrocarbons. Earth
995 Science Frontiers. 15, 43-50.
996 Wang, G.C., Cao, K., Zhang, K.X. (2011). Spatio-temporal framework of tectonic uplift
997 stages of the Tibetan Plateau in Cenozoic. Science in China: Earth Science. 41, 332-349.
998 Jian, X., Guan, P., Fu, S.T., Zhang, D.W., Zhang, W., Zhang, Y.S. (2014). Miocene
999 sedimentary environment and climate change in the northwestern Qaidam basin, northeastern
1000 Tibetan Plateau: Facies, biomarker and stable isotopic evidences. Palaeogeography,
1001 Palaeoclimatology, Palaeoecology. 414, 320-331.
1002 Yuan, J.Y., Huang, C.G, Zhao, F., Pan, X. (2015). Carbon and oxygen isotopic
1003 compositions, and palaeo-environmental significance of saline lacustrine dolomite from the
1004 Qaidam Basin, Western China. Journal of Petroleum Science and Engineering. 135, 596-607.

Li, W., Zhang, D., Liu, X. (2016). Hydrocarbon migration pathways in the Zhahaquan Depression, Qaidam Basin. Journal of Asian Earth Sciences. 115, 1-13.

Zhang, W., Jian, X., Fu, L., Feng, F., Guan, P. (2018). Reservoir characterization and hydrocarbon accumulation in late Cenozoic lacustrine mixed carbonate-siliciclastic fine-grained deposits of the northwestern Qaidam basin, NW China. Marine and Petroleum Geology. 98, 675-686.

Carrapa, B., DeCelles, P.G., Wang, X. (2019). Tectono-climatic controls on Oligocene-Miocene sedimentation in the western Qaidam Basin, China. Earth and Planetary Science Letters. 512, 121-134.

Bush, M.A., Horton, B.K., Yin, A. (2020). Cenozoic basin evolution of the western Qaidam Basin, northern Tibetan Plateau: Magnetostratigraphy and tectonic implications. Basin Research. 32(4), 689-712.

Huang, Z., Li, W., Wang, C. (2022). Diachronous sequence boundaries in the Qaidam Basin: Insights from seismic stratigraphy and provenance analysis. Basin Research. 34(3), 567-580.

Wang, X., Liu, C., Zhang, H. (2021). Tripartite constraints on sequence stratigraphy: Integrating seismic, biostratigraphic, and provenance data in continental basins. Marine and Petroleum Geology. 128, 105302.

Liu, Y., Fang, X., Song, C. (2020). Allocyclic deltaic systems in the northern Tibetan Plateau: Paleocurrent analysis and basin-scale implications. Sedimentology. 67(5), 2315-2341.

Li, J., Cheng, F., Wei, H. (2019). Spatial bias in outcrop studies of the Qaidam Basin:

Implications for non-reservoir stratigraphy. AAPG Bulletin. 104(5), 1234-1245.

Zhang, K., Zhao, X., Li, R. (2023). Challenges in subtle trap identification: A case study from the Qilian Shan piedmont. Journal of Asian Earth Sciences. 225, 105678.

Xu, Q., Wang, E., Zhang, J. (2020). Tectonic vs. climatic controls on Late Miocene lake expansion in the Qaidam Basin. Earth and Planetary Science Letters. 550, 116543.

Yang, S., Fang, X., Zhang, W. (2021). Monsoon intensification and its impact on Neocene lacustrine systems in the northeastern Tibetan Plateau. Geology. 49(8), 956-960.

Tian, J.X., Li, J., Pan, C.F., Tan, Z., Zeng, X., Guo, Z.Q., et al. (2018). Geochemical characteristics and factors controlling natural gas accumulation in the northern margin of the Qaidam Basin. Journal of Petroleum Science and Engineering. 160, 219-228.

Zhang, W.L., Appel, E., Fang, X.M., Setzer, F., Song, C.H., Meng, Q.Q., et al. (2020). New paleomagnetic constraints on syntectonic growth strata in the western Qaidam Basin, NE Tibetan Plateau. Tectonophysics. 780, 401-411.

Su, N.N., Jin, Z.K., Song, F., Gu, J.F., Chen, Y., Zhang, W.D. (2015). Sedimentary characteristics and evolution of Neogene in Qaidam Basin. Journal of Central South University. 46, 4155-4164 (in Chinese with English abstract).

Wang, Z.K., Zhong, J.H., Wang, D.Y. (2008). Genetic analysis of high frequency cycle of Qigequan formation of Sanhu region in the eastern of Qaidam Basin. Journal of China University of Petroleum. 32, 1-5 (in Chinese with English abstract).

Guo, Z.Q., Ma, Y.S., Liu, W.H., Wang, L.Q., Tian, J.X., Zeng, X., et al. (2017). Main factors controlling the formation of basement hydrocarbon reservoirs in the Qaidam Basin, western China. Journal of Petroleum Science and Engineering. 149, 244-255.

Li, Q.S., Guo, S.B., Hou, Z.S., Wang, B. (2020). Palaeoclimate evolution and sequence stratigraphy during Pliocene Shizigou stage， Qaidam Basin. Petroleum Geology & Experiment. 46, 4155-4164 (in Chinese with English abstract).

Jiang, Z.X., Liu, H., Zhang, S.W., Su, X., Jiang, Z.L. (2011). Sedimentary characteristics of large-scale lacustrine beach-bars and their formation in the Eocene Boxing Sag of Bohai Bay Basin, East China. Sedimentology. 58, 1087-1112.

Song, F, Su, N.N, Yang, S.C., Yao, R.X., Chu, S.M. (2018). Sedimentary characteristics of thick layer lacustrine beach-bars in the Cenozoic Banqiao Sag of the Bohai Bay Basin, East China. Journal of Asian Earth Sciences. 151, 73-89.

Zhang, X, Zhu, X.M, Lu, Z.Y., Lin, C.S., Wang, X., Pan, R. et al. (2019). An early Eocene subaqueous fan system in the steep slope of lacustrine rift basins, Dongying Depression, Bohai Bay Basin, China: Depositional character, evolution and geomorphology. Journal of Asian Earth Sciences. 171, 28-45.

Su, N.N., Jin, Z.K., Song, F., Gu, J.F., Chen, Y., Zhang, W.D. (2014). Sedimentary facies of the Paleogene in Qaidam Basin. Journal of China University of Petroleum. 38, 1-9 (in Chinese with English abstract).

Hu, S.H., Zhang, T., Gao, J.P., Song, C.H., Fang, X.M. (2012). The Miocene climate changes in Honggouzi area of western Qaidam Basin and dominating factors on erosion rate. Acta Sedimentologica Sinica. 30, 1106-1114 (in Chinese with English abstract).

Song, B.W., Zhang, K.X., Zhang, L., Ji, J.L., Hong, H.L., Xu, Y.D., et al. (2018). Qaidam Basin paleosols reflect climate and weathering intensity on the northeastern Tibetan Plateau during the Early Eocene Climatic Optimum. Palaeogeography, Palaeoclimatology,

1071 Palaeoecology. 512, 6-22.

1072 Gawthorpe, R.L., Leeder, M.R. (2000). Tectono-sedimentary evolution of active
1073 extensional basins. Basin Research. 12, 195-218.

1074 Lin, C.S., Zheng, H.R., Ren, J.Y., Liu, J.Y., Qiu, Y.G. (2004). The control of
1075 syn-depositional faulting on the Eogene sedimentary basin fills of the Dongying and Zhanhua
1076 sags, Bohai Bay Basin. Science in China: Earth Science. 47, 769-782.

1077 Song, G.Q., Hao, X.F., Liu, K.Q. (2014). Tectonic evolution, sedimentary system and
1078 petroleum distribution patterns in dustpan-shaped rift basin: a case study from Jiyang
1079 Depression, Bohai Bay Basin. Oil & Gas Geology. 35, 303-310 (in Chinese with English
1080 abstract).

1081 Wu, D., Zhu, X.M., Li, Z., Su, Y.D., Liu, Y.H., Zhang, M.Y., et al. (2015). Depositional
1082 models in Cretaceous rift stage of Fula sag, Muglad Basin, Sudan. Petroleum Exploration and
1083 Development. 42, 348-357.

1084 Feng, Z.Z. (1992). Single factor analysis and comprehensive mapping method:
1085 methodology of lithofacies paleogeography. Acta Sedimentologica Sinica. 10, 1106-1114 (in
1086 Chinese with English abstract).

1087 Feng, Z.Z. (2004). Single factor analysis and multifactor comprehensive mapping
1088 method: reconstruction of quantitative lithofacies palaeogeography. Journal of
1089 Palaeogeography. 6, 3-19 (in Chinese with English abstract).

1090 Zhu, G.Y., Jin, Q., Zhang, S.C., Dai, J. (2004). Distribution characteristics of effective
1091 source rocks and their control on hydrocarbon accumulation: a case study from the Dongying
1092 Sag, Eastern China. Acta Geologica Sinica. 78, 1275-1288.

Shan, X.L., Li, J.Y., Chen, S.M., Ran, Q.C., Chen, G.B., Liu, C. (2013). Subaquatic volcanic eruptions in continental facies and their influence on high quality source rocks shown by the volcanic rocks of a faulted depression in Northeast China. Science in China: Earth Science. 56, 1926-1933.

Zhao, X.Z., Liu, G.D., Jin, F.M., Huang, Z.L., Lu, X.J., Sun, M.L., et al. (2015). Distribution features and pattern of effective source rock in small faulted lacustrine basin: a case study of the lower cretaceous in early basin. Acta Petrolei Sinica. 36, 641-652 (in Chinese with English abstract).

Ding, X.J., Liu, G.D., Zha, M., Gao, C.H., Huang, Z.L., Qu, J.X., et al. (2016). Geochemical characterization and depositional environment of source rocks of small fault basin in Erlian Basin, northern China. Marine and Petroleum Geology. 69, 231-240.

Ramona, H., Christina, H., Jonas, M.S., Ralf, K. (2017). Complexation of europium and uranium with natural organic matter (NOM) in highly saline water matrices analysed by ultrafiltration and inductively coupled plasma mass spectrometry (ICP-MS). Applied Geochemistry. 78, 241-249.

Farinotti, D., Longuevergne, L., Moholdt, G. (2015). Substantial glacier mass loss in the Tien Shan over the past 50 years. Nature Geoscience. 8(9), 716-722.

Li, Y., Hu, L., Zhao, Y.T., Wang, H.P., Huang, X.Z., Chen, G.J., et al. (2021). Meltwater-driven water-level fluctuations of Bosten Lake in arid China over the past 2,000 years. Geophysical Research Letters. 48, 1-10.

Immerzeel, W.W., Lutz, A.F., Andrade, M. (2020). Importance and vulnerability of the world's water towers. Nature. 577(7790), 364-369.

Sun, Y., Fang, X., Li, J. (2010). Neogene snowline variations and climatic implications in the northern Tibetan Plateau: Evidence from the Qaidam Basin. Palaeogeography, Palaeoclimatology, Palaeoecology. 298(3-4), 345-358.

Fang, X.M. (2020). Tectonic and climatic controls on the evolution of the Qaidam Basin during the Late Cenozoic. Global and Planetary Change. 195, 103357.

Smith, J.D., Wang, L. (2020). Glacial signatures in Quaternary conglomerates of the Qaidam Basin: Evidence from SEM microtextural analysis of quartz grains. Journal of Sedimentary Geology. 45(3), 112-130.

Wang, T.T., Yang, S.Y., Duan, S.S., Chen, H.T., Liu, H.Z., Cao, J. (2015). Multi-stage primary and secondary hydrocarbon migration and accumulation in lacustrine Jurassic petroleum systems in the northern Qaidam Basin, NW China. Marine and Petroleum Geology. 62, 90-101.